Extended Linear Path Space Model and its Application: Static-Dynamic Hedging in Managing the Risk of Variable Annuities

By

Yoon Seok Choi

Doctoral Student

Hanyang University

cys9202@dreamwiz.com

Supervisor: Sang Bin Lee

Professor of Finance

Hanyang University

Seoul, Korea

May 2006

Abstract

Variable annuities have grown tremendously in recent years, offering life insurers significant growth opportunities. These equity and interest rate structured products offer a broad range of guarantees to the policyholders, and insurers must manage their risks.

The insurer's risk management program must consider modeling and implementation challenges beyond that of the standard capital market approach. This paper proposes solutions to six significant issues: (1) computational efficiency, (2) impact of equity returns and interest rate correlations on the cost of guarantee, (3) uncertain surrendering of policies and withdrawal of account value, (4) internal transfer of funds, (5) suboptimal exercise of options, and (6) a cost/benefit analysis of a hedging program.

These solutions are extended from the traditional capital market approach. Specifically, in this paper, I describe the fair valuation of the guarantees using a three factor model incorporating interest rate and equity risks. Then I use the Linear Path Space methodology to simulate and value the risks. Finally, I simulate the effectiveness of using a combined static-dynamic hedging program in dealing with the practical considerations mentioned above.

Keywords: variable annuities, static-dynamic hedging, key rate duration, linear path space, insurer's risk management, guaranteed minimum benefits

A. Introduction

Variable annuities are retirement products sold by insurance companies to individuals, qualified and non-qualified accounts. The insurance companies manage the retirement contributions over a period of time, the accumulation period, for a fee in their separate accounts. Each policyholder at the end of the accumulation period can choose to receive the account value or a specified annuity. But, insurers also offer "riders" to this basic product.

Insurers offer their policyholders guarantees in these products such as the Guaranteed Minimum Death Benefits (GMDB), the Guaranteed Minimum Account Value (GMAV), the Guaranteed Minimum Withdrawal Benefits (GMWB), and the Guaranteed Minimum Income Benefits (GMIB). In practice, the variable annuities often have combinations of these guarantees with many variations to the basic design.

Consider GMIB as an example. The variable annuities offer the policyholder the option of receiving the account value or an annuity at the end of the accumulation period. This option leads to a complex mix of equity and interest rate risks embedded in the guarantee.

Insurers bear the risks of these guarantees and must manage such risks on their balance sheet. Therefore a methodology to measure and manage the risks of these guarantees is an important issue. To date, research has focused on treating the guarantees of the variable annuities as financial products, using the standard value sensitivities (the greeks) to measure and manage their risks (Milevsky and Promislow (2001), Boyle and Hardy (2003) and Wilkie et al. (2003)). An alternative approach is static hedging. One method constructs a portfolio of tradable derivatives that matches the payoffs of the guarantee of a fixed annuity (Pelsser (2003)). Another method, pathwise immunization, uses a portfolio of equity and interest rate options that matches the pathwise values of the guarantees (Ho and Mudavanhu (2005a)). However, these approaches do not address some of the key practical considerations for an insurer to implement a hedging program.

The purpose of this paper is to fill this void. This paper proposes solutions to six significant issues: (1) computational efficiency, (2) impact of equity returns and interest rate correlations on the cost of the guarantee, (3) uncertain surrendering of policies and withdrawal of account value, (4) a cost/benefit analysis of a hedging program, (5) suboptimal exercise of options, and, (6) alternative to equity funds and internal transfer of funds.

Our method uses the capital market approach. Specifically, in this paper, we describe the fair valuation of the guarantees using a three factor model incorporating interest rate and equity risks. We extend the generalized two factor Ho-Lee model, an arbitrage-free interest rate model, to incorporate an equity return factor. The valuation model is then used to value a Guaranteed Minimum Income Benefit (GMIB), under a range of correlations between the equity returns and the yield curve level and slope movements.

To enhance the computational efficiency, we propose the extended Linear Path Space methodology that combines interest rate and equity risks to simulate and value the GMIB risks. We then describe a combined static-dynamic hedging program that deals with the efficiency of the hedging program. The dynamic hedging program is based on using the key rate durations and delta. Finally, we extend the basic model in the paper to describe some solutions to the remaining practical considerations.

The main results of the paper are summarized as follows. (1) The GMIB value is estimated to be 13.42% of the account value. The hedging portfolio of equity and bond options can hedge the GMIB effectively, even though the GMIB has an embedded option with a stochastic strike price. (2) The residual risk from the pathwise immunization is relatively small, only $1.28 total absolute amount used in hedging $14.69 of GMIB on a $100 account value. The mismatch of the key rate durations of the GMIB and the option hedging portfolio can be managed by dynamic hedging using swaps and actively traded bonds. (3) The correlations between the yield curve movements and the equity return risk can significantly affect the guaranteed value. The correlations of the equity returns with the yield curve movements may account for 9.5% of the GMIB value. In particular, a hedging program must recognize the significant impact of the steepening movement of the yield curve on the GMIB value. (4) The suboptimal exercise of options can be modeled by incorporating transaction cost, using the methodology used in modeling prepayments in mortgage-backed securities valuation. (5) The value-at-risk by scenarios of a GMIB can be measured by the pathwise values of the LPS valuation.

The paper proceeds as follows. Section B describes the valuation model of a GMIB. While we use a GMIB in this paper for the analysis, the method can be extended to other guarantees of variable annuity. Section C describes the GMIB modeling using LPS and discusses the computational efficiency and the issues with equity correlations to the yield curve movements. Section D presents a static-dynamic hedging strategy and describes its application to managing the product risks and to structuring a cost/benefit analysis of a hedging program. Section E describes other extensions of the basic model that would incorporate the suboptimal exercise of options and non-equity investment funds. Section F contains the conclusions, suggesting the broad implications of the results.

B. A Model of a Guaranteed Minimum Income Benefit (*GMIB*)

The valuation model is based on a combined interest rate and equity return model. The model is related to Kishimoto (1989) which provides a two dimensional recombining lattice model that relates the Ho-Lee one factor model (1986) with an equity return process. Our interest rate model is the generalized Ho-Lee two factor interest rate model and the equity returns are not recombining, as the equity returns are modeled as a lognormal distribution and not a binomial distribution.

There are many types of guaranteed minimum income benefits (GMIB) of a variable annuity. In this paper, we describe only the salient features of the guarantee that is relevant to the paper. The GMIB model is based on Ho and Mudavanhu (2005a). For the completeness of the presentation, we briefly describe the model here that highlights the economic assumptions.

1. Market Assumptions

Our model assumes that the GMIB and the variable annuity can be viewed as standard contingent claims on the market interest rate and equity risks. Specifically, the assumption enables us to show that the variable annuity and GMIB fair values are directly and instantaneously related to the market risks, and therefore, they can be replicated by market instruments.

For the interest rate model, we assume a two-factor arbitrage-free model (Ho-Lee (2005)), represented in the continuous time formulation here:

$$\mathrm{d}r = \theta(r,t)\mathrm{d}t + \sigma_{r1}(r,t)\mathrm{d}W_1 + \sigma_{r2}(r,t)\mathrm{d}W_2 \tag{1}$$

$\theta(r, t)$ depends on the initial spot yield curve and the term structure of volatilities. $\sigma_{r1}(r, t)$ and $\sigma_{r2}(r, t)$ are the term structure volatilities of the interest rate model. Each of the volatilities has the behavior that

$$\sigma_{ri}(r,t) = \begin{cases} \sigma_i(t)R & when\ r > R \\ \sigma_i(t)r & when\ r < R \end{cases} \tag{2}$$

$\sigma_i(t)$ is a continuous function of t for $i = 1,2$. R is called the threshold rate, a real number. When the short-term rate exceeds threshold rate, the model is normal for that risk factor. Conversely, when the short rate falls below the threshold rate, the model is lognormal.

We use this two-factor Ho-Lee model (2005) to model the interest rate risk for analyzing the variable annuities because this model fulfills the following requirements. First, the Ho-Lee model is arbitrage-free enabling us to relative value the contingent claims. Second, this model behaves lognormally when interest rates are low. Third, the two-factor model enables us to decouple the equity one period expected returns, which must equal the short-term rate, from the long rate, which determines the annuity value. Any one-factor model assuming the short rate to be perfectly correlated with the long rate would be problematic for modeling GMIB. Fourth, the Ho-Lee model is not a lognormal model, in that the interest rates do not grow exponentially. Unacceptably high interest rates would lead to unrealistic expected instantaneous equity returns. Fifth, recently Ho and Mudavanhu (2005b) have shown that the model is robust empirically, providing significant explanatory power to the observed prices of a broad range of traded swaptions. The specification of the generalized Ho-Lee model is provided in Appendix A for the completeness of the exposition.

We assume that the variable annuity invests in an equity index and the equity return process follows a lognormal process under the risk neutral martingale process given by the standard equation.

$$\frac{dS}{S} = r\mathrm{d}t + \sigma\left(\rho_1 \mathrm{d}W_1 + \rho_2 \mathrm{d}W_2 + \sqrt{1-\rho_1^2-\rho_2^2}\,\mathrm{d}Z\right) \tag{3}$$

S is the value of the index. r and σ are the instantaneous risk free returns and standard deviation of the index respectively. dZ, dW_1 and dW_2 are the independent standard Wiener processes. ρ_1 (ρ_2) is the correlation coefficient between equity returns and the first (second) factor of interest rate movements of the generalized Ho-Lee model. The first factor can be described as the "steepening movement" where the short term rate moves more than the long term rate. The second factor is the parallel movement where the entire yield curve shifts in a parallel fashion. Also note that the two factors of generalized Ho-Lee model are independent of each other.

2. The Variable Annuity with the GMIB

We assume that the variable annuity is a single premium product. The policyholder pays a premium P initially. The premium is invested in an equity index S. The fee of the variable annuity is paid continuously, and it is a constant proportion f of the account value. Let V be the account value. Then

$$\mathrm{d}V = \mathrm{d}S - fV\mathrm{d}t \tag{4}$$

At the end of the accumulation period, T, the policyholder can elect to receive the account value or a zero coupon bond, with maturity T^*. We use a zero coupon bond instead of an annuity, equal payments over a period of time, for the clarity of exposition. A zero coupon bond can capture the impact of interest rate risks of the variable annuity. We further assume that the policyholders have no mortality risk, do not lapse or seek partial withdrawal. We will consider lapsation later in the paper. These simplifying assumptions do not affect the results of the analysis because the mortality risk is not related to market risks. Finally, we assume that the policyholders maximize their wealth. Specifically, the payoff to the policyholder at the end of the accumulation period is given by the maximum of the account value and the bond (the fixed annuity) value:

$$\mathrm{Max}[V(T), B(T, T^*)] \tag{5}$$

where $V(T)$ and $B(T, T^*)$ are the values of the account and the zero coupon bond with maturity T^* at time T respectively.

Our model seeks to capture the key features of the option embedded in the GMIB, which is the equity put option feature with a stochastic strike price. The stochastic behavior is driven by the interest rate uncertainty, affecting the fixed annuity value.

3. Valuation Model

The valuation model is based on the discrete time framework. Specifically, we use a monthly step size to value the variable annuity and the GMIB.

The return of the index is given by a lognormal process with an expected return r, the risk free rate under the "risk neutral assumption" and an instantaneous volatility of σ over a one month period. Let $S(n)$ be the index value at time n, where each time period is one month, then by discretizing Equation (3) we get

$$\begin{aligned} &S(n+\Delta t; i, j) \\ &= S(n; i, j)\exp\left\{\left(r(n; i, j) - 0.5\sigma^2\right)\Delta t + \sigma\left(\rho_1\varepsilon_1 + \rho_2\varepsilon_2 + \sqrt{1-\rho_1^2-\rho_2^2}\,\varepsilon_Z\right)\sqrt{\Delta t}\right\} \end{aligned} \tag{6}$$

Given the yield curve and the interest rate volatility surface, the two-factor interest rate lattice can be specified according to Appendix A. Given a random interest rate path taken from the interest rate lattice model, the values ε_1 and ε_2 from the interest rate lattice are known. The value of ε_1 or ε_2 is +1 or -1, depending on the outcome of the risk factors from time n to time n+1. The value of ε_Z is drawn from $N \sim (0, 1)$. Equation (6) provides a path of the equity index value. The set of interest rates and the equity value for each path is called a scenario. Note that the returns of the account value are locally correlated to the interest rate factors as specified by Equation (6).

The valuation of the variable annuity begins with the specification of the account value along a scenario path. Let $V(n; i, j)$ be the account value at time n, the value at the end of the nth period and at the state (i, j). Then, the account value at the end of the period is based on the equity returns on $V(n; i, j)$ net of the fees. Combining Equation (3) and Equation (4), the account value process is given by[1]:

$$\frac{\mathrm{d}V}{V} = \left(r - f\right)\mathrm{d}t + \sigma\left(\rho_1\mathrm{d}W_1 + \rho_2\mathrm{d}W_2 + \sqrt{1-\rho_1^2-\rho_2^2}\,\mathrm{d}Z\right) \tag{7}$$

and can be discretized as:

$$\begin{aligned} &V(n+\Delta t; i, j) \\ &= V(n; i, j)\exp\left\{\left(r(n; i, j) - f - 0.5\sigma^2\right)\Delta t + \sigma\left(\rho_1\varepsilon_1 + \rho_2\varepsilon_2 + \sqrt{1-\rho_1^2-\rho_2^2}\,\varepsilon_Z\right)\sqrt{\Delta t}\right\} \end{aligned} \tag{8}$$

A scenario path of the account value is generated by the procedure described in Equation (6). Equation (8) is then used to simulate the terminal account value at time T[2].

By the specification of the variable annuity product, the initial account value is the premium P:

$$V(0) = P \tag{9}$$

[1] See Appendix D for more explanation of Equation (7).

[2] See Appendix E for the local conditional distribution of the account value process given two-factor interest rate model.

And at the termination of the accumulation period, since the policyholder seeks to maximize the value of his/her holdings, the insurer must pay to the policyholder,

$$Y(i, j) = \mathrm{Max}[B(T, T^*; i, j) - V(T; i, j), 0] \qquad (10)$$

where B is the fair value of the "annuity" and V is the account value at time T.

Note that the policyholders, on the other hand, receives in all states,

$$Z(i, j) = \mathrm{Max}[V(T; i, j), B(T, T^*; i, j)] \qquad (11)$$

And

$$V(T; i, j) = Z(i, j) - Y(i, j), \qquad (12)$$

That is, the sum received by the policyholder $Z(i, j)$ together with the payout of the insurer $Y(i, j)$ has to equal the account value at the termination date.

The valuation of the variable annuity and the GMIB proceeds as follows. First, we generate the interest rate and equity return scenarios. Then, for each scenario, we use Equation (8) to generate the path of the account value. As a result, we can determine the fee for each month generated from the account value along each scenario. The present value of the fees net of the guarantee cost for each path is called the pathwise value. This cashflow is discounted along the corresponding interest rate path, using the short term rate of each one month period (the step size of the lattice). The average of the pathwise values over the scenarios is the value of the variable annuity. The average of the pathwise values of the guaranteed amount according to Equation (10) is the value of the GMIB.

C. Valuing a GMIB using the LPS methodology: Computational Efficiency and Correlation Risk

This section provides the procedure in valuing the GMIB using the LPS methodology. Our approach is similar to Lesseig and Stock (1998) and (2000) where the LPS scenarios are used to value and analyze corporate bonds with default risks. However, their model is based on Kishimoto (1989) recombining lattice, while we construct the LPS scenarios from the model described in the previous section. The LPS model is described elsewhere (Ho (1992), Lee and Choi (2005) and Lesseig and Stock (1998)). For the completeness of the exposition, the detailed construction of the LPS scenarios is described in Appendix B and the key steps are described below to specify the notations and terminologies.

1. LPS Valuation Method

Step 1: Determine the equivalent class and the representative paths from the two-factor interest rate LPS model.

We use five term-segments of 12th, 36th, 60th, 84th, and 120th month. The states of the world at each segment are partitioned into "gates". The total number of the representative paths of the two-factor interest rate is 59,049 ($=3^{5\times 2}$), since we use the five term segments and the two-factor interest rate model.

The set of paths that pass through the same set of gates defines an equivalent class. For each equivalent class of paths, we define that "representative" path that has the average behavior of the paths in that equivalent class.

A representative path can be denoted by a vector. The vector elements are (n, i, j) where n is the period and i (j) is the upward movements of the first (second) factor at period n. The number of the upward movements determines the states at each period.

Step 2: Calculate the one-period discount factor on a representative path of the two-factor interest rate LPS model.

From the interest rate model, we have the one-period discount factor specified as follows.

$$P_{i,j}^{n}(1)=\frac{P(n+1)}{P(n)}\prod_{k=1}^{n}\left(\frac{1+\delta_{0,1}^{k-1}(n-k)}{1+\delta_{0,1}^{k-1}(n-k+1)}\right)\prod_{k=1}^{n}\left(\frac{1+\delta_{0,2}^{k-1}(n-k)}{1+\delta_{0,2}^{k-1}(n-k+1)}\right)\prod_{k=0}^{i-1}\delta_{k,1}^{n-1}(1)\prod_{k=0}^{j-1}\delta_{k,2}^{n-1}(1) \qquad (13)$$

Explanation of Equation (13) is given in Appendix A. Since a representative path can be denoted by (n, i, j) and the one-period discount factor is a function of n, i, and j, we can calculate the one-period discount function corresponding to each step of a representative path. There are 120 steps for each representative path since we use a monthly step size for the 10-year GMIB.

Step 3: Calculate the probability for each representative path.

Since a representative path represents a set of paths in an equivalent class, we assign the weight of the equivalent class as the probability of the representative path. We calculate the number of paths in each equivalent class and divide it by the total number of paths considered. The sum of probabilities of the representative paths must therefore equal to one.

Once we have the probabilities of the one-factor interest rate LPS, we cross-multiply the probabilities of the one-factor interest rate LPS to determine the probabilities of the two-factor interest rate LPS, because the two factors in the interest rate movements are independent each other.

Step 4: Simulate the GMIB payoffs conditional on the selected representative interest paths.

We simulate the account value, V, 100 times per each selected interest rate representative path using Equation (8). Since we simulate the price paths of the account value conditional upon each interest rate representative path, we use the movements of the interest rate representative paths. Therefore, we only simulate ε_Z from $N \sim (0, 1)$. The total random array of ε_Z per each selected interest rate representative path is 100 by 120 since there are 120 time periods per each interest rate representative path and we simulate 100 times per each interest rate path.

The arithmetic average of the 100 terminal GMIB payoffs in Equation (10), which is $\Sigma Y(i,j)/100$, is the GMIB payoff corresponding to each selected interest rate representative path.

Step 5: Determine the pathwise values.

In this paper, we choose the first 500 most probable representative paths out of 59,049 ($=3^{5\times2}$) paths to value the GMIB valuation. Since the sum of all the selected representative path probabilities is not equal to one, we again divide the 500 representative path probabilities by the sum of 500 representative path probabilities, to normalize the probabilities. Step 4 has determined the cashflow for each representative path. Therefore, we can determine the present value of the cashflow along that particular scenario path. That present value is called the pathwise value. In this step, we have determined 500 pathwise values.

Step 6: Calculate the GMIB value.

The value of the GMIB is the weighted sum of the pathwise values, weighted by the probabilities of the interest rate paths.

2. *Numerical Simulation Results*

The simulation results assume the market parameters on July, 2005. The yield curve is based on the ISDA mid-market par swap rates[3], which is {3.94, 4.08, 4.22, 4.3, 4.36, 4.41, 4.49, 4.6, 4.87} in % in year {0, 1, 2, 3, 4, 5, 7, 10, 30} respectively where the rate at time 0 is an extrapolated value. We use the implied volatility functions specified by Ho-Mudavanhu (2005b) based on the volatility surface described in Table 1. In their empirical test, they have shown that this specification provides significant explanatory power to the market observed swaption prices. The implied volatility functions are: $\sigma_1(t) = (0.417 + 0.061t)\exp(-0.132t)$ and $\sigma_2(t) =$ 0.154 for all t. The threshold rate is assumed to be 3%.

Table 1. Swaptions volatility surface given by the Black volatilities quoted (in %).

	Swap Tenor (years)									
Option Term (years)	1yr	2yr	3yr	4yr	5yr	6yr	7yr	8yr	9yr	10yr
1yr	44.40	36.50	32.90	29.70	27.60	25.70	25.40	24.00	23.40	23.30

[3] Data: http://www.federalreserve.gov/releases/h15/data.htm

2yr	31.20	28.80	27.10	25.30	24.20	22.90	23.00	21.80	21.30	21.10
3yr	27.00	25.30	24.30	23.10	22.20	21.30	21.10	20.40	20.00	19.90
4yr	24.00	22.80	21.90	21.20	20.70	19.90	19.70	19.10	18.70	18.60
5yr	22.30	21.30	20.80	19.90	19.40	18.70	18.50	18.00	17.70	17.40
7yr	19.80	19.10	18.50	18.10	17.60	16.90	16.70	16.30	16.00	15.80
10yr	17.40	16.40	15.90	15.60	15.10	14.50	14.50	14.10	13.90	13.70

The equity volatility σ is assumed to be 20%.

Table 2 reports the 10-year at-the-money simulated GMIB values with a 3% fee over a range of correlations, and Figure 1 shows the GMIB performance profiles over different correlations and account values.

Table 2. At-the-money GMIB values for different correlations with the account value 100

ρ_1	0.0	0.5	0.0	0.5	-0.5	0.0	-0.5	0.5	-0.5
ρ_2	0.0	0.0	0.5	0.5	0.0	-0.5	-0.5	-0.5	0.5
GMIB	14.69	17.46	16.79	19.59	10.87	11.98	7.49	14.90	13.13

The simulation of the GMIB values provides five interesting observations.

a. The GMIB value is significant. The simulation result shows that the guarantee ranges 7.5% to 20% of the account value, and that is the present value cost to the general account. The profitability of selling the variable annuity product is the present value of the fees, net of this guarantee and the present value of the operating costs.
b. A positive correlation of equity returns to the yield curve movement leads to a higher GMIB value. Consider columns 1, 4, and 7. Note that the GMIB is a mix of an equity put option and a bond call option. When the yield curve falls, the underlying asset value increases. And when the correlation is positive, the lower rates would likely leads to a lower equity value, and in turn the equity put option would be deeper in-the-money, leading to a higher option value. Conversely, if the correlation of the equity returns to the yield curve movement is negative, then the higher bond option payoff at a lower interest rate level is offset by the rise in the equity value, resulting to the lower equity option payoff. In this case, equity and interest rate risk are offsetting each other in valuing the GMIB.
c. The impact of positive correlation is lower than that of the negative correlation. Consider columns 4 and 7. The results show that the increase of the GMIB value with the positive correlation is lower than that of the decrease in value with a negative correlation of the same magnitude. This asymmetric behavior can be explained by the option behavior, which shows that the natural hedge between the equity and the annuity obligation has significant impact on the GMIB value with a negative correlation.
d. The correlation to the steepening yield curve movement has a greater impact than that to the level movement. Consider columns 2, 3, 5, 6. The worst scenario for the insurer's GMIB position is when the yield curve falls and steepens as the equity market falls. In this case, not only the annuity obligation has the higher

value as the equity put option becomes deeper in the money, the instantaneous return of the equity is also smaller, as the short rate falls.

e. Using the historical data, the correlations of the equity returns to the parallel shift and the steepening shift are estimated to be -0.287 and 0.032[4]. The GMIB value for these correlations is \$13.42. Therefore, when we ignore the impact of correlations, we tend to overstate the GMIB value by \$1.27, or 9.5%.

The combined effect of the above five observations implies that if the equity return is positively related to both yield curve movements, as in the case with the equity broad based index in a recession scenario, then the GMIB value is significant. When the account value is at-the-money, the correlations may raise the GMIB value by 33% (=(19.59-14.69)/14.69). Conversely, if the correlations are negative, then the GMIB value may lower by 49% (=(14.69-7.49)/14.69).

Figure 1. GMIB performance profiles for different correlations and account values

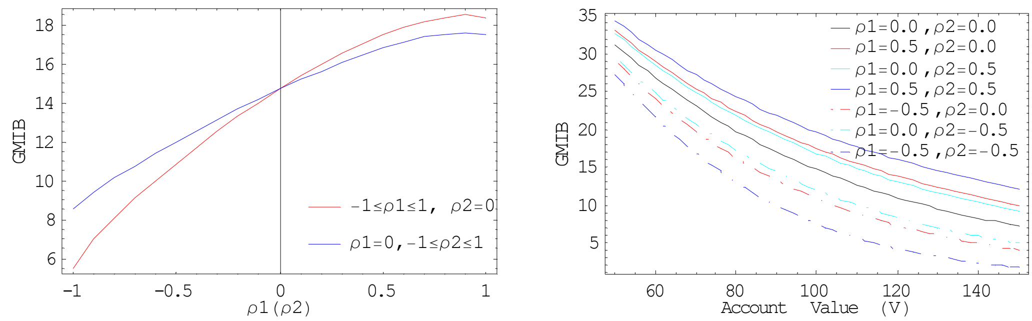

The left panel of Figure 1 depicts the performance profiles of the at-the-money GMIB for different correlations of ρ_1 and ρ_2 while the right panel shows the performance profiles of GMIB over a range of account values given seven combinations of correlations.

This section provides insights into two practical considerations. First, a hedging program of a block of variable annuity business involves intensive computation. The LPS methodology can provide the scenario simulations with computational efficiency.

[4] We use ISDA mid-market par swap rates with maturity of {1, 2, 3, 4, 5, 7, 10, 30} in order to implement PCA of yield curve dynamics. The sample period is from 2000/08 to 2005/07. The first three eigenvalues are {7.17, 0.74, 0.07} and their cumulative weight are {0.897, 0.989, 0.998} respectively. The corresponding eigenvectors shows level, slope and curvature factors as in other literature. Each principal component being the time series of transformed data variables weighted by the corresponding eigenvector, we can estimate the correlation of S&P index returns to both the first principal component, related with the parallel shift and the second principal component, related with the steep shift. See Lardic, Priaulet, and Priaulet (2001) for a discussion on the comparison of the methodologies of PCA. Also see Appendix C for estimates of correlation coefficients between stock index and the first two principal components of yield curve dynamics.

Second, the simulation results show that the correlation of the equity returns and the yield curve movements have significant implications to the GMIB value. The result suggests that the chosen equity portfolio of a variable annuity with GMIB has a significant impact on the guarantee value. If the equity portfolio is more recession protected, then, the equity return may in fact provide a natural hedge to the annuity value. Many GMIB hedging program focuses on using capital market instruments to hedge the market risk. This simulation result shows that the design of the variable annuities may even have a greater effect in minimizing the guarantee risks.

D. Static-Dynamic Hedging: Managing Product Risks and Identifying Potential Loss

Suppose the scenarios cover all the possible paths in the one factor lattice. Ho and Chen (1997) show that if two securities have the same pathwise values and have the same cash flow along the forward curve, then they must also have the same cashflow along each path of the lattice. That is, the two securities are identical according to the lattice model.

Intuitively, suppose that two securities have the same pathwise values for a large set of scenarios in the lattice, and further suppose that the lattice approximates the scenarios in the real world. Then, if we reinvest any cash at the prevailing one period interest rate at each node, the two securities must have the same future value at some distant future. And in this sense, the two securities are equivalent. The decomposition methodology seeks to determine a portfolio of securities that is equivalent to the structured product. This portfolio is constructed from a predetermined set of benchmark securities.

This section begins by using the pathwise immunization methodology of Ho and Mudavanhu (2005a) but applying the LPS methodology. To determine the initial set of benchmark securities to construct the replicating portfolio of the GMIB, we begin with investigating the embedded options in the GMIB.

To replicate the embedded options, we use equity put options on an equity index and bond call options with different strike prices but the same expiration date, the end of the accumulation period. Specifically, let the index k = 1, …, 500 denote the scenarios. Equity_Put(X, k) and Bond_Call(X', k) denote the pathwise value of the put option on equity and the call option on bond with strike price X and X' for scenario k, respectively. Then we seek to determine the optimal portfolio of the hedging instruments such that the portfolio of which can replicate the GMIB, on the pathwise basis. That is,

$$\begin{aligned} &GMIB(k) \\ &= a + b(1)\times Bond\_Call(X_1,k) + b(2)\times Bond\_Call(X_2,k) + \cdots + b(m)\times Bond\_Call(X_m,k) \\ &\quad + c(1)\times Equity\_Put(X_1',k) + c(2)\times Equity\_Put(X_2',k) + \cdots + c(n)\times Equity\_Put(X_n',k) + \varepsilon(k) \end{aligned} \tag{14}$$

The pathwise values of the GMIB and the hedging instruments are calculated. We can use a regression to determine the coefficients. The value of the intercept a is the cash value in \$, since cash has a constant value under all scenarios. The coefficients $b(i)$ and

$c(j)$ (i =1,…,m; and j = 1,…,n) are the position sizes of the hedging instruments used in the hedging portfolio.

To search for the optimal hedging portfolio, a stepwise regression is used. The stepwise regression is a technique for choosing the variables, i.e., terms, to include in a multiple regression model. In particular, we use the backward stepwise regression, which starts with all model terms available[5]. At each step it deletes the most statistically insignificant term (the one with the lowest *t*-statistic or highest *p*-value) until only the statistically significant terms left. This iterative process allows us to identify the hedging instruments that can have the most explanatory power to the GMIB's pathwise values.

1. Results of the Decomposition of GMIB

In this section, we represent the GMIB as a portfolio of equity and bond options. Using the decomposition method described above, the decomposition of the GMIB as a portfolio of the hedging instruments is presented in Table 3 below.

Table 3. Decomposition of the GMIB with a 3% annual fee

A	B	C	D	E	F	G	H	I
Hedging Instrument	Strike	Fair Value	Regression Coeffs.	t-statistics	Dollar value	Delta	Duration	Dollar Duration
Cash	-	1.00	3.32	4.97	3.32	0.00	0.00	0.00
Bond Call	10	57.20	-0.19	-10.20	-10.81	0.00	21.41	-231.43
Bond Call	20	50.90	-0.16	-10.25	-8.11	0.00	22.78	-184.87
Bond Call	30	44.61	-0.11	-10.33	-4.82	0.00	24.54	-118.25
Bond Call	40	38.31	-0.02	-6.51	-0.73	0.00	26.87	-19.57
Bond Call	50	32.01	0.14	9.20	4.41	0.00	30.13	132.72
Bond Call	60	25.71	0.42	9.71	10.84	0.00	34.98	379.22
Bond Call	80	13.94	0.33	12.35	4.62	0.00	50.85	234.92
Bond Call	100	5.42	0.28	12.95	1.54	0.00	69.42	107.12
Bond Call	120	1.53	0.17	8.69	0.26	0.00	87.96	22.57
Equity Put	40	0.14	1.56	4.04	0.22	-0.01	53.54	11.71
Equity Put	100	6.98	0.37	5.22	2.55	-0.16	32.86	83.86
Equity Put	150	22.55	0.51	14.88	11.40	-0.35	26.07	297.28
Replicating Portfolio					14.69	-0.24	48.68	715.26
GMIB					14.69	-0.22	48.34	710.09

Column A identifies the hedging instruments used in the decomposition. All the equity put options expire in 10 years. The bond call options, expiring in 10 year also, are options on the 20 year zero-coupon bond therefore the time to maturity of the underlying bond is 10 years at option expiration. The underlying bond face value is set such that the bond forward value with delivery in year 10 (the expiry term) is 100. Column B provides all

[5] In the numerical example below, we assume that all the available hedging instruments are composed of thirteen bond call options with strikes {10, 20, …, 120, 130} and nineteen equity put options with strikes {20, 30, …, 190, 200}.

the strike prices of the options. Column C is the fair value of the hedge instrument, Column D regression coefficients are interpreted as the numbers of hedging instruments required for the replication. Column E presents the t-statistics showing the importance of the hedging instrument in the replication. Column F shows the dollar value of each hedging instrument, the replicating portfolio and GMIB. The dollar value of each hedging instrument is the product of the fair value and regression coefficient. The sum of all the dollar values of hedging instruments is the value of replicating portfolio. Column G shows the delta of each hedging instrument, the replicating portfolio and GMIB. The delta of replicating portfolio is the sum of product of each delta and corresponding regression coefficient in Column D. Column H shows the duration of each hedge instrument, replicating portfolio and GMIB. The duration of replicating portfolio ($Duration_P$) is calculated as follows:

$$Duration_P = \sum_{i=1}^{13} \left(\frac{H_i}{P} \right) Duration_i \tag{15}$$

where P is the value of replicating portfolio, H_i is the dollar value of hedge instrument i and $Duration_i$ is the duration of hedge instrument i. We assume that yield curve shifts 10 basis points in computing the durations. Column I shows the dollar duration of each hedging instrument, replicating portfolio and GMIB. Dollar duration is the product of duration and dollar value of each hedging instrument. The sum of dollar duration of all the hedging instruments is the dollar duration of replicating portfolio.

The total value of the GMIB is \$14.69 on a \$100 account value. The risk profile at the time of evaluation of the GMIB can be summarized as follows. The equity risk is equivalent to holding a short position of \$22 in equity. The interest rate risk is equivalent to holding a long position of \$14.69 in a bond with a duration of 48.34 years. Of course, this risk profile changes in time.

The R^2 of 99% suggests that the hedging fits the pathwise values of the GMIB quite well. Indeed, considering the replicating portfolio has a duration of 48.68 year versus the GMIB duration of 48.34 year, the results shows that the pathwise immunization can result in matching the duration. The decomposition results are quite intuitive. Given the interest rate risks, the "strike price" of the equity put option is a bond value which must necessarily be stochastic given the interest rate uncertainty. This is reflected by the use of equity put options with strike prices 40, 100 and 150. Also, we have discussed that GMIB is exposed to the interest rate risk, particularly when the interest rates are low. This is captured by the in-the-money bond call option with strikes 10, 20, 30, 40, 50, 60 and 80, at-the-money bond call option with a strike price of 100 and out-of-the-money bond call option with a strike price of 120.

To provide better insights into the effectiveness of the decomposition, Figure 2 depicts the scattered plots of the GMIB pathwise values against those of the replicating portfolio. The results show that the residuals are not proportional to the size of the pathwise values and therefore the replication is effective even for the "worse scenarios" (high GMIB pathwise values) where the insurers have to pay more benefits.

Figure 2. Scattered plot of fitted GMIB pathwise values against GMIB pathwise values

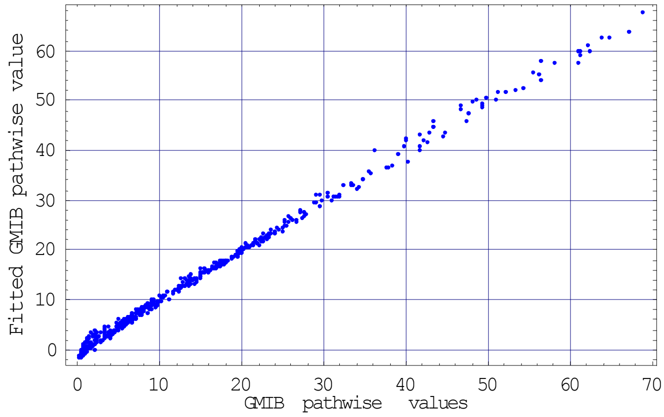

2. Static-Dynamic Hedging

In this section, we calculate the key rate durations of the hedged positions. And then we use swaps and equity to conduct the dynamic hedging. The key rate durations (KRD) of the GMIB shows that the value of the guarantee is sensitive to the yield curve shape movements.

Table 4 presents key rate durations and the dollar key rate durations of GMIB and the replicating portfolio. These sensitivity measures enable us to determine the dynamic hedging, which is required to ensure that the combined dynamic and static hedging strategies can replicate the GMIB with minimal hedging cost.

Table 4. Key Rate Duration and Dollar Key Rate Duration Matching

	Cash	Bond Call	Bond Call	Bond Call	Bond Call	Bond Call	Bond Call	Bond Call	Bond Call	Bond Call	Equity Put	Equity Put	Equity Put	GMIB
Strike	-	10	20	30	40	50	60	80	100	120	40	100	150	100
Dollar Value	3.32	-10.81	-8.11	-4.82	-0.73	4.41	10.84	4.62	1.54	0.26	0.22	2.55	11.40	14.69
1	0.00	-0.04	-0.04	-0.04	-0.04	-0.04	-0.04	-0.05	-0.06	-0.07	-0.17	-0.11	-0.09	-0.09
2	0.00	0.02	0.02	0.02	0.02	0.02	0.03	0.03	0.05	0.06	0.51	0.16	0.09	0.13
3	0.00	-0.01	-0.01	-0.01	-0.01	-0.01	-0.01	-0.01	0.04	0.06	0.31	0.04	0.00	0.05
4	0.00	0.03	0.03	0.03	0.03	0.03	0.03	0.04	0.08	0.09	0.45	0.17	0.11	0.17
5	0.00	0.04	0.04	0.04	0.04	0.05	0.05	0.07	0.16	0.21	0.62	0.21	0.13	0.22
7	0.00	0.12	0.12	0.12	0.13	0.13	0.14	0.20	0.53	1.28	0.34	0.29	0.24	0.40
10	0.00	10.22	10.22	10.22	10.22	10.22	10.22	10.09	8.73	5.70	51.50	32.14	25.61	23.81
30	0.00	11.04	12.41	14.16	16.49	19.74	24.57	40.48	59.81	80.91	0.00	0.00	0.00	23.68
Sum KRD*	0.00	21.43	22.80	24.55	26.89	30.14	34.99	50.85	69.35	88.23	53.56	32.90	26.10	48.37
Dur**	0.00	21.41	22.78	24.54	26.87	30.13	34.98	50.85	69.42	87.96	53.54	32.86	26.07	48.34

* KRD = key rate duration

** Dur = duration

	$KRD (Hedge)	$KRD (GMIB)	Net $KRD	P(t)	r(t)	Duration of ZCB*	$Amount Needed
1	-1.328	-1.324	0.003	0.980	0.020	0.980	0.003
2	1.641	1.970	0.329	0.947	0.027	1.947	0.169
3	0.336	0.734	0.398	0.904	0.034	2.902	0.137
4	1.868	2.441	0.573	0.858	0.038	3.852	0.149
5	2.480	3.267	0.787	0.812	0.042	4.800	0.164
7	4.795	5.930	1.135	0.721	0.047	6.687	0.170
10	352.651	349.756	-2.895	0.598	0.051	9.511	-0.304
30	353.120	347.879	-5.241	0.172	0.059	28.339	-0.185
Sum	715.563	710.652					0.302

* ZCB = zero coupon bond

The upper panel of Table 4 shows the key rate durations of hedge portfolio and GMIB. Consider the key rate durations of the GMIB. It shows that the cost of the guarantee is most sensitive to the 30-year rate with the value rises when the 30-year rate falls for bond calls and most sensitive to the 10-year (option expiration) rate for equity puts. The sum of key rate durations approximately equals the duration, showing that the structured sampling of the interest rate scenarios is quite adequate. The lower panel shows the dollar key rate durations ($KRD) of hedge portfolio and GMIB, net dollar key rate durations (Net$KRD), initial discount function (P(t)), initial yield curve (r(t)), duration of zero coupon bond and the amount needed of zero coupon bond for dynamic hedge.

The dollar key rate duration of hedge portfolio for maturity t ($\$KRD_P(t)$) is calculated as follows:

$$\$KRD_P(t) = \sum_{i=1}^{13} \$Value_i \times KRD_i(t) \tag{16}$$

where $\$Value_i$ is the dollar value of hedge instrument i and $KRD_i(t)$ is the key rate duration of hedge instrument i respectively.

GMIB value is $14.69 and the dollar key rate durations ($KRD) of GMIB are the multiplication of these values by the key rate durations respectively. The net dollar key rate durations (Net$KRD) are the differences between the dollar key rate durations of GMIB and replicating portfolio. Note that, because of the effectiveness of the pathwise immunization, the net $key rate duration is relatively small.

To remove the key rate duration mismatch, we construct the hedge portfolio of zero-coupon bonds, which have the same net dollar key rate durations. The amounts required to replicate the net dollar key rate duration is the net dollar key rate duration over the duration of T-year zero-coupon bond. The total $ amount needed for the zero-coupon bonds is $0.3. The total absolute $ amount involved in the dynamic hedging is only $1.28

on the \$14.69 GMIB value. In addition, a long position of \$2 equity will minimize the difference of deltas between GMIB and replicating portfolio in Column F of Table 3.

The results show that the dollar value of the dynamic hedging position is much lower. Further this dynamic hedging position can avoid using options or swaptions, which typically have higher transaction costs. Further, since the equity and bond options used match the pathwise values of the GMIB, we have also minimized the vega risks of the equity option as well as the vega risk of bond option embedded in the GMIB.

3. Use of the Static-Dynamic Hedging Strategy to Manage the Product Risk and the Cost/Benefit Analysis

Ho-Mudavanhu (2005a) shows that the static hedge can reduce transaction costs. Further, the method can hedge the vega risks in the equity and the interest rate options, since the volatilities of the equity returns and the interest rate risk are themselves stochastic (Ho-Mudavanhu (2005b)). For this reason, dynamic hedging fails to manage these long dated option risks because dynamic hedging assumes constant volatility (Derman and Taleb (2005)).

However, static hedging requires the embedded GMIB be invariant, and such is not the case with the presence of product risks. Given the uncertainty of lapsation, either with the surrendering of the policy or the withdrawal of the account value, the book value of the GMIB may decrease.

The proposed static-dynamic hedging approach can be used to manage such product risks. Assumptions can be made on the stochastic behavior of the lapsation and the withdrawal behavior. The stochastic model can then be introduced to Step 4 in the valuation procedure. Additional pathwise values are generated taking these additional stochastic factors into account. Then the static hedging is formulated taking these additional risks into account. The remaining risk is then managed by the dynamic hedging as part of the asset and liability management program, continually adjusting to the expected level of future lapsation and withdrawals.

The results of this section also suggest a cost/benefit tradeoff analysis. The cost of a hedging program is the transaction cost, which can be estimated by the turnover of the trading. The benefit would be the reduction of the risk exposure. Therefore, the cost/benefit of a hedging program begins with the measure of the reduction of risk and the turnover of trade of alternative hedging strategies. Note that the weighted average of the pathwise values is the fair value of a contingent claim. The pathwise value can be interpreted as the present value of the cashflow along that scenario on a risk-adjusted basis (Ho-Lee (2004, pp.592)). This suggests that the distribution of the pathwise value of a GMIB is a measure of the risk exposure to the insurer.

Specifically, Step 5 enables us to determine the distribution of the pathwise values of a GMIB. The hedging program will then determine the portion of the distribution to be managed by static hedging and the portion to be managed by dynamic hedging. The insurer may accept the risk of the extreme tail of the distribution because the events are too improbable and the cost of which may be too costly. Or, the insurer may also take part of the risk of more probable events because the risk and return tradeoff warrants such a position when the insurer is taking a market view. Our approach can measure the reduction of the risks under a particular hedging program by identifying the distribution of the pathwise values before and after putting on the hedging.

E. Extending the Basic Model: Suboptimal Exercise of Options and Alternative Funds

Thus far we have presented the basic GMIB model. However, the model can be extended to incorporate other features of variable annuities. We will consider two such examples here.

1. Suboptimal Exercise of Options

Many variable annuities' design depends on the policyholders, which may be targeted as hot or cold money. The value of the GMIB is significantly affected by the target policyholders. Hot money would exercise their options efficiently while the cold would not.

This policyholder behavior is analogous to that of the mortgagors in prepaying or refinancing their mortgages as interest rates fall. Some mortgagors would refinance their mortgages as soon as that is economically optimal, while others may not. Research in mortgage-backed securities valuation uses transaction costs in the option model to capture this effect.

Specifically, let $C > 0$ be the transaction cost which is positively related to the coldness of the money. The perfectly hot money would have zero transaction cost. Then Equation (10) is replaced by:

$$Y(i,j) = \begin{cases} B(T,T^*;i,j) - V(T;i,j) & \text{if} \quad B(T,T^*;i,j) - V(T;i,j) > C \\ 0 & \text{otherwise} \end{cases} \tag{17}$$

In this case, the policyholder would not annuitize in some states of the world even if it is profitable to do so. Insurer can incorporate a range of transaction cost levels to reflect the coldness of the money and its impact on the GMIB value. Or the model can be adjusted for the cases where policyholders annuitize when it is not optimal to do so.

2. Alternative Investments of the Variable Annuities

We have described the variable annuities based on investing in equity. In Section C, we have discussed the importance of using alternative equity funds in the variable annuities because of the fund returns correlation to the yield curve risks. However, we have modeled only the equity funds.

The model can be adjusted to deal with bond funds. In this case, the equity return in Equation (6) is replaced by the bond return equation. The bond returns can be determined by the generalized Ho-Lee model for a particular duration structure of the bond fund. There is no equity risk in this case, and the bond return is completely determined by the yield curve risk, and therefore, the generalized Ho-Lee model that specifies the entire yield curve at each node point can determine the bond fund returns at each node point.

To be realistic, of course, a bond fund would have other risks, basis risks, prepayment risks or credit risks, for example. But such additional risk can also be added to the model. To the extent that some funds are balance funds. Then Equation (6) would be replaced by a linear combination of the equity return model and a bond return model. Furthermore, policyholders can make internal transfer of funds in an unexpected way, then such risks can be measured and managed as we have discussed in the product risk section.

Note that, in Section C, we have argued the importance of the negative correlation of the fund returns to the yield curve risk. This analysis shows that if the fund is a long term bond fund, then the bond fund returns would be highly negatively correlated with the yield curve risks. Then the natural hedge within the variable annuity would be greatest, resulting in minimal GMIB value, or minimal risk exposure to the insurer.

F. Conclusions

This paper describes an effective and practical method to manage the GMIB. In particular, we use a combined static-dynamic hedging strategy to manage the risks. We show that the GMIB is sensitive to the yield curve shape movements and that the interest rate risk has to be managed by both the delta and the key rate durations. Further, we have used the extended LPS method to provide a computationally efficient method to determine the optimal hedging strategy. We then show that this approach can be applied to deal with six practical considerations in implementing a hedging program of the variable annuities.

While this paper has applied the method to manage the GMIB risks, the methodology presented should have broad applications. It can be applied to other variable annuity risks. Further, the method can be used for managing pension liabilities. Pension liabilities are often represented by a cash flow stream of fixed payments. The assets supporting the liabilities are often equities. For this reason, the downside scenario for the pension plan is the precipitous fall in the equity returns along with a fall in interest rates. And therefore, the pension sponsor would seek to manage an option similar to the GMIB. The method presented can be used to manage the downside risk of such a pension plan. Furthermore, the pension liabilities are also often uncertain and have long duration, with characteristics similar to the problem discussed in this paper. And therefore, the solutions discussed in this paper for the practical considerations can also be applied to the pension plan management.

Appendix A: Generalized Ho-Lee Model

The one-factor generalized Ho-Lee model

The building blocks of the binomial model are the binormal volatilities δ_i^n, for $0 \le i \le n$. δ_i^n is the proportional decrease in the one period bond value from state *i* to *i*+1 at time *n*+1. Without loss of generality, we assume that the bond price decreases, and the bond yield increases, with state *i*, and hence $\delta_i^n < 1$. When $\delta_i^n = 1$, by definition, there is no risk at the binomial node with respect to the upstate and downstate outcomes.

$$\delta_i^n = \frac{P_{i+1}^{n+1}}{P_i^{n+1}} \text{ for all } n,\ 0 \le n \le N-1 \text{ and } 0 \le i \le n \tag{A.1}$$

But there are several requirements imposed on these binomial volatilities.

Condition 1: State dependent volatility requirement asserts that the proportional change of one period bond price is proportional to the interest rate level when the rates are low, constant when it is high.

To specify Condition 1, we begin with the definition of the one period yield:

$$R_i^n = -\log P_i^n / \Delta t, \tag{A.2}$$

where Δt is the time interval of one period. For example, if one binomial period (the step size of the lattice) is one month, then Δt is 1/12.

According to Equation (A.1), we have

$$\log \delta_i^n = -\log P_i^{n+1} + \log P_{i+1}^{n+1} \tag{A.3}$$

Substituting Equation (A.2) into (A.3), we have

$$\log \delta_i^n = (R_i^{n+1} - R_{i+1}^{n+1})\Delta t \tag{A.4}$$

By the market convention, interest rate volatilities are the standard deviations of proportional change in the annualized yields of the bonds. Let σ_i^n be the annualized volatility at time *n* and state *i*, noting that the difference of the two binomial outcomes is two standard deviations, then we have:

$$R_{i+1}^{n+1} - R_i^{n+1} = 2\sigma_i^n R_i^n \sqrt{\Delta t} \tag{A.5}$$

Substitution $R_{i+1}^{n+1} - R_i^{n+1}$ of Equation (A.5) into (A.4), and simplify, we derive the relationship of the binomial volatilities and the market convention of interest rate volatilities.

$$\delta_i^n = \exp\left(-2\sigma_i^n R_i^n \Delta t^{3/2}\right) \tag{A.6}$$

Equation (A.6) presents the one-to-one relationship between δ_i^n and $\sigma_i^n R_i^n$. Let R be some fixed interest rate level, which we call the threshold rate, independent of both n and i. We now assume that on the one hand, the interest rate movement is lognormal when $R_i^n < R$, and therefore σ_i^n is a function of n, denoted by $\sigma(n)$ and not the states i. On the other hand, we assume that the interest rate movement becomes normal when $R_i^n > R$, evolving from the lognormal process to the normal process continuously. And therefore, $\sigma_i^n R_i^n$ is independent of the state i, and equals $\sigma(n)R$. This motivates the following specification of σ_i^n,

$$\sigma_i^n R_i^n = \sigma(n)\min\left(R_i^n, R\right) \tag{A.7}$$

$\sigma(n)$ is some continuous function of time n, which can be interpreted as the term structure of volatilities. By substitution of Equation (A.7) into Equation (A.6), we have the following specification of the forward volatilities:

$$\delta_i^n = \exp\left(-2\sigma(n)\min\left(R_i^n, R\right)\Delta t^{3/2}\right) \tag{A.8}$$

We further assume that the function $\sigma(n)$ is specified by some parameters a, b, c, and d, which can be obtained from the calibration to the market price of swaption.

$$\sigma(n) = (a + bn)\exp\left(-cn\right) + d \tag{A.9}$$

The specification of the term structure of volatilities is motivated by the observed market volatility curve. The volatility curve tends to decay exponentially with a term linearly related to time, with a hump in the short to intermediate term at times. Equation (A.8) and (A.9) are important in specifying the arbitrage-free interest rate model. Equation (A.8) ensures interest rates are non-negative and non-explosive, and Equation (A.9) ensures the mean-reversion behavior.

Condition 2. Arbitrage-free condition

The arbitrage-free yield curve movements condition applies to all the bonds with different maturities T, we therefore need to consider the binomial volatilities with another dimension T, $\delta_i^n(T)$. Specifically,

$$\delta_i^n(T) = \frac{P_{i+1}^{n+1}(T)}{P_i^{n+1}(T)} \qquad 0 \le T \tag{A.10}$$

That is, the binomial volatility is the proportion of the T-year bond at (i+1)th state to the ith state at time n+1. Note that, $\delta_i^n(0) = 1$, because the one-period bond has no uncertainties over one period. The volatility for one period bond is $\delta_i^n(1) = \delta_i^n$, which are given numbers for the time being.

Figure A.1. Recombining Binomial Tree

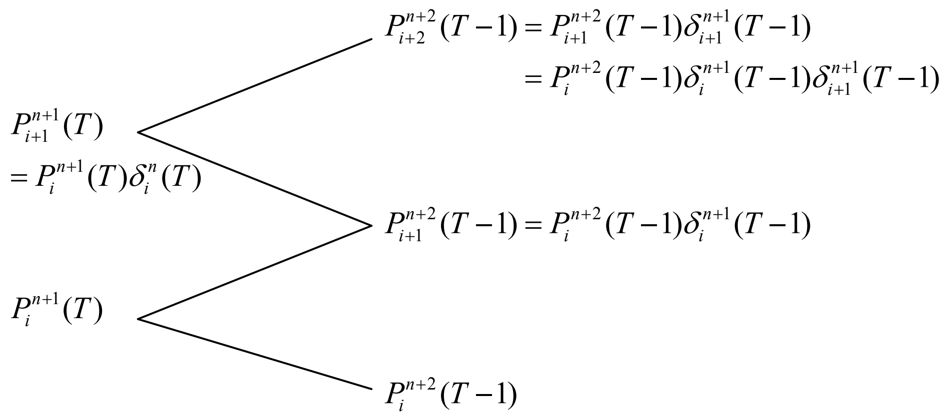

Proposition 1: The arbitrage-free condition requires the volatility to be as follows:

$$\delta_i^n(T) = \delta_i^n(1)\delta_i^{n+1}(T-1)\left(\frac{1+\delta_{i+1}^{n+1}(T-1)}{1+\delta_i^{n+1}(T-1)}\right) \tag{A.11}$$

Proof 1:

By Harrison and Kreps,

$$\begin{aligned} P_i^{n+1}(T) &= P_i^{n+1}(1)\frac{1}{2}\left(P_i^{n+2}(T-1) + P_{i+1}^{n+2}(T-1)\right) \\ &= P_i^{n+1}(1)\frac{1}{2}P_i^{n+2}(T-1)\left(1+\delta_i^{n+1}(T-1)\right) \end{aligned} \tag{A.12}$$

where we used Equation (A.10) and using the similar way,

$$\begin{aligned} P_{i+1}^{n+1}(T) &= P_{i+1}^{n+1}(1)\frac{1}{2}\left(P_{i+1}^{n+2}(T-1) + P_{i+2}^{n+2}(T-1)\right) \\ &= P_{i+1}^{n+1}(1)\frac{1}{2}P_i^{n+2}(T-1)\delta_i^{n+1}(T-1)\left(1+\delta_{i+1}^{n+1}(T-1)\right) \end{aligned} \tag{A.13}$$

Dividing Equation (A.13) by (A.12) gives us the desired result as follows:

$$\frac{P_{i+1}^{n+1}(T)}{P_i^{n+1}(T)} = \frac{P_{i+1}^{n+1}(1)}{P_i^{n+1}(1)} \delta_i^{n+1}(T-1) \frac{\left(1+\delta_{i+1}^{n+1}(T-1)\right)}{\left(1+\delta_i^{n+1}(T-1)\right)}$$

$$\Updownarrow$$

$$\delta_i^n(T) = \delta_i^n(1)\delta_i^{n+1}(T-1)\frac{\left(1+\delta_{i+1}^{n+1}(T-1)\right)}{\left(1+\delta_i^{n+1}(T-1)\right)}$$

Q. E. D.

Equation (A.11) defines the relationships of the binomial volatilities of T-year bonds, and is important to the construction of the arbitrage-free rate model.

Note that if the binomial volatilities are independent of states, but dependent on time, then the above condition implies that:

$$\delta^n(T) = \delta^n \delta^{n+1} ... \delta^{n+T-1} \tag{A.14}$$

When the binomial volatilities are both state and time independent, then

$$\delta^{n+1}(T) = \delta^T, \tag{A.15}$$

where T is the power and not a superscript.

Equation (A.14) and (A.15) are used in Ho-Lee (2004) and Ho-Lee (1986) respectively. Therefore Equation (A.11) shows that this model is a generalization of the previous models.

Given the above conditions, Proposition 2 shows the bond pricing model for the T-period bond price at node (n, i).

Proposition 2: Given the Proposition1, the bond pricing formula for the T-period bond price in state i and time n is:

$$P_i^n(T) = \frac{P(n+T)}{P(n)} \prod_{k=1}^{n} \left(\frac{1+\delta_0^{k-1}(n-k)}{1+\delta_0^{k-1}(n-k+T)} \right) \prod_{j=0}^{i-1} \delta_j^{n-1}(T) \tag{A.16}$$

Proof 2:

From Equation (A.10), we already know that

$$P_i^n(T) = P_0^n(T) \prod_{j=0}^{i-1} \delta_j^{n-1}(T) \tag{A.17}$$

So it suffices to check that

$$P_0^n(T) = \frac{P(n+T)}{P(n)} \prod_{k=1}^{n} \left(\frac{1+\delta_0^{k-1}(n-k)}{1+\delta_0^{k-1}(n-k+T)} \right) \tag{A.18}$$

We use the mathematical induction in order to prove Proposition 2. It is simple to show that Equation (A.18) holds for $n = 1$.

$$\begin{aligned} P(1+T) &= P(1)\frac{1}{2}\left(P_0^1(T) + P_1^1(T)\right) \\ &= P(1)\frac{1}{2}P_0^1(T)\left(1+\delta_0^0(T)\right) \\ P_0^1(T) &= \frac{P(1+T)}{P(1)} \frac{2}{\left(1+\delta_0^0(T)\right)} \end{aligned} \tag{A.19}$$

Therefore, Equation (A.18) holds for $n = 1$ since $\delta_i^n(0) = 1$ by definition.

Now we hypothesize that Equation (A.18) holds for arbitrary time n. Then,

$$\begin{aligned} P_i^n(T+1) &= P_i^n(1)\frac{1}{2}\left(P_{i+1}^{n+1}(T) + P_i^{n+1}(T)\right) \\ \frac{P_i^n(T+1)}{P_i^n(1)} &= \frac{1}{2}P_0^{n+1}(T)\left(\prod_{j=0}^{i}\delta_j^n(T) + \prod_{j=0}^{i-1}\delta_j^n(T)\right) \\ &= \frac{1}{2}P_0^{n+1}(T)\prod_{j=0}^{i-1}\delta_j^n(T)\left(1+\delta_i^n(T)\right) \end{aligned} \tag{A.20}$$

By the way,

$$\begin{aligned} P_i^n(T+1) &= P_0^n(T+1)\prod_{j=0}^{i-1}\delta_j^{n-1}(T+1) \text{ by equation (A.17)} \\ &= \frac{P(n+T+1)}{P(n)}\prod_{k=1}^{n}\left(\frac{1+\delta_0^{k-1}(n-k)}{1+\delta_0^{k-1}(n-k+T+1)}\right)\prod_{j=0}^{i-1}\delta_j^{n-1}(T+1) \text{ by induction hypothesis.} \end{aligned} \tag{A.21}$$

And in a similar way,

$$\begin{aligned} P_i^n(1) &= P_0^n(1)\prod_{j=0}^{i-1}\delta_j^{n-1}(1) \quad \text{by equation (A.17)} \\ &= \frac{P(n+1)}{P(n)}\prod_{k=1}^{n}\left(\frac{1+\delta_0^{k-1}(n-k)}{1+\delta_0^{k-1}(n-k+1)}\right)\prod_{j=0}^{i-1}\delta_j^{n-1}(1) \quad \text{by induction hypothesis} \end{aligned} \tag{A.22}$$

Dividing Equation (A.21) by (A.22) is

$$\frac{P_i^n(T+1)}{P_i^n(1)}=\frac{P(n+T+1)}{P(n+1)}\prod_{k=1}^{n}\left(\frac{1+\delta_0^{k-1}(n-k+1)}{1+\delta_0^{k-1}(n-k+T+1)}\right)\prod_{j=0}^{i-1}\left(\frac{\delta_j^{n-1}(T+1)}{\delta_j^{n-1}(1)}\right) \tag{A.23}$$

Finally, equating the RHS of Equation (A.20) and the RHS of Equation (A.23) gives us the desired result that, by induction hypothesis, Equation (A.18) holds automatically at time n+1 as follows:

$$\frac{1}{2}P_0^{n+1}(T)\prod_{j=0}^{i-1}\delta_j^n(T)\left(1+\delta_i^n(T)\right)=\frac{P(n+1+T)}{P(n+1)}\prod_{k=1}^{n}\left(\frac{1+\delta_0^{k-1}(n-k+1)}{1+\delta_0^{k-1}(n-k+T+1)}\right)\prod_{j=0}^{i-1}\left(\frac{\delta_j^{n-1}(T+1)}{\delta_j^{n-1}(1)}\right) \tag{A.24}$$

Rearrange Equation (A.24) as follows:

$$\begin{aligned}
P_0^{n+1}(T)&=\frac{P(n+1+T)}{P(n+1)}\prod_{k=1}^{n}\left(\frac{1+\delta_0^{k-1}(n-k+1)}{1+\delta_0^{k-1}(n-k+T+1)}\right)\prod_{j=0}^{i-1}\left(\frac{\delta_j^{n-1}(T+1)}{\delta_j^{n-1}(1)\delta_j^n(T)}\right)\frac{2}{\left(1+\delta_i^n(T)\right)}\\
&=\frac{P(n+1+T)}{P(n+1)}\prod_{k=1}^{n}\left(\frac{1+\delta_0^{k-1}(n-k+1)}{1+\delta_0^{k-1}(n-k+T+1)}\right)\prod_{j=0}^{i-1}\left(\frac{1+\delta_{j+1}^n(T)}{1+\delta_j^n(T)}\right)\frac{2}{\left(1+\delta_i^n(T)\right)} \quad \text{by (A.11)}\\
&=\frac{P(n+1+T)}{P(n+1)}\prod_{k=1}^{n}\left(\frac{1+\delta_0^{k-1}(n-k+1)}{1+\delta_0^{k-1}(n-k+T+1)}\right)\frac{2}{1+\delta_0^n(T)} \quad \text{by cancellations}\\
&=\frac{P(n+1+T)}{P(n+1)}\prod_{k=1}^{n+1}\left(\frac{1+\delta_0^{k-1}(n+1-k)}{1+\delta_0^{k-1}(n+1-k+T)}\right) \quad \text{by using the fact that } \delta_0^n(0)=1
\end{aligned} \tag{A.25}$$

Now that we have checked Equation (A.18) holds for arbitrary n, the proof of Equation (A.16) is complete.

Q. E. D.

The two-factor generalized Ho-Lee model

Let $P_{i,j}^n(T)$ be the price of a T year bond at time n, at state (i, j). Then the bond price is specified by combining two one-factor models. Specifically, we have

$$P_{i,j}^n(T)=\frac{P(n+T)}{P(n)}\prod_{k=1}^{n}\left(\frac{1+\delta_{0,1}^{k-1}(n-k)}{1+\delta_{0,1}^{k-1}(n-k+T)}\right)\prod_{k=1}^{n}\left(\frac{1+\delta_{0,2}^{k-1}(n-k)}{1+\delta_{0,2}^{k-1}(n-k+T)}\right)\prod_{k=0}^{i-1}\delta_{k,1}^{n-1}(T)\prod_{k=0}^{j-1}\delta_{k,2}^{n-1}(T) \tag{A.26}$$

where

$$\begin{aligned}\delta_{i,1}^{n}(T) &= \delta_{i,1}^{n}\delta_{i,1}^{n+1}(T-1)\left(\frac{1+\delta_{i+1,1}^{n+1}(T-1)}{1+\delta_{i,1}^{n+1}(T-1)}\right)\\ \delta_{i,2}^{n}(T) &= \delta_{i,2}^{n}\delta_{i,2}^{n+1}(T-1)\left(\frac{1+\delta_{i+1,2}^{n+1}(T-1)}{1+\delta_{i,2}^{n+1}(T-1)}\right)\end{aligned} \tag{A.27}$$

and the one period forward volatilities are given by definition,

$$\begin{aligned}\delta_{i,1}^{n}(1) = \delta_{i,1}^{n} &= \exp\left(-2\cdot\sigma_1(n)\min\left(R_{i,1}^{n},R\right)\Delta t^{3/2}\right)\\ \delta_{i,2}^{n}(1) = \delta_{i,2}^{n} &= \exp\left(-2\cdot\sigma_2(n)\min\left(R_{i,2}^{n},R\right)\Delta t^{3/2}\right)\end{aligned} \tag{A.28}$$

where the functions $\sigma_j(n) = (a+bn)\exp\left(-cn\right)+d$ is specified by the parameters a, b, c, and d, which can be obtained from the calibration to the market price of swaption.

Using the direct extension, we can specify the one period rates for the two-factor model for any future period n and state i, and $R_{i,1}^{n}$ and $R_{i,2}^{n}$ are defined by

$$\begin{aligned}R_{i,1}^{n}\Delta t &= -\log\left(\frac{P(n+1)}{P(n)}\right)-\sum_{k=1}^{n}\log\left(\frac{1+\delta_{0,1}^{k-1}(n-k)}{1+\delta_{0,1}^{k-1}(n-k+1)}\right)-\sum_{k=0}^{i-1}\log\left(\delta_{k,1}^{n-1}(1)\right)\\ R_{i,2}^{n}\Delta t &= -\log\left(\frac{P(n+1)}{P(n)}\right)-\sum_{k=1}^{n}\log\left(\frac{1+\delta_{0,2}^{k-1}(n-k)}{1+\delta_{0,2}^{k-1}(n-k+1)}\right)-\sum_{k=0}^{i-1}\log\left(\delta_{k,2}^{n-1}(1)\right)\end{aligned}. \tag{A.29}$$

Appendix B: Linear Path Space Method

In this appendix, we describe a structured sampling method of the interest rate and equity scenarios. Specifically, we specify a sample of interest rate scenarios with assigned probability weight to each scenario. This sample can represent the path space defined by the binomial lattice. For each interest rate scenario, we then determine a random sample of the equity returns, which are specified by the interest rate scenario.

Figure B.1 shows the partitioning of the path space. We first divide the term from 0 to 10 years into segments consistent with the key rates at year {1, 3, 5, 7, 10} when the time horizon considered is 10 years. The i^{th} term segment, $T(i)$ is the i^{th} key rate year multiplied by 12 in monthly step size. The set of all term segments is therefore a vector of {12, 36, 60, 84, 120}. The length of the i^{th} segment is defined as $L(i)=T(i)-T(i-1)$, $T(0)=1$. There are five segments. The first segment is (0, 11), the second (12, 35), …, and the fifth is (84, 119).

Figure B.1. Linear Path Space

term segment T(i)	T(i)−1	Partitioning of the Path Space										
1	0						(0,0)					
12	11					(0,3)	(4,7)	(8,11)				
36	35				(0,11)	(12,15)	(16,19)	(20,23)	(24,35)			
60	59			(0,11)	(12,23)	(24,27)	(28,31)	(32,35)	(36,47)	(48,59)		
84	83		(0,11)	(12,23)	(24,35)	(36,39)	(40,43)	(44,47)	(48,59)	(60,71)	(72,83)	
120	119	(0,17)	(18,29)	(30,41)	(42,53)	(54,57)	(58,61)	(62,65)	(66,77)	(78,89)	(90,101)	(102,119)

↑ center segment of the ith Key State Space

The state space at the end of each segment is called the key state space. The first key state space has twelve states (0 ~ $T(1)$–1), the second has thirty-six (0 ~ $T(2)$–1), etc. We then generate the key state space partition recursively to be consistent with level scenarios and symmetric up and down scenarios. We divide the first key state space into three equal partitions (up, level, down): (0, 3), (4, 7), (8, 11). In partitioning the second state space, we need to keep the first partition the same as the second to ensure that there are level rate movements. Then the remaining states on both ends of the second state space become the remaining partitions. Hence the thirty-six states of the second key state space are partitioned into five parts. For the K^{th} key state space, there are $2K+1$ partitions.

Next we define the recursive generation of linear partitioning. Given the K^{th} key space partition, the $(K+1)^{th}$ key space partition, beyond the first partition (0, $[T(K+1)-T(K)]/2$ -1), creates the second and following partitions up to the $2(K+1)^{th}$ partitions simply by adding $[T(K+1)-T(K)]/2$ to all the entries to the K^{th} partition. The $2(K+1)+1^{th}$ partition is $([T(K+1)+T(K)]/2,\ T(K+1)-1)$.

There are 1×3×5×...×11 equivalent classes, but many of them have no rate path belonging to the equivalent class. The linear path space considers only the equivalent classes where rate paths go up, stay level, or go down to another scenario node, and therefore they stay relatively stable within each term segment. As a result, there are 3^5 equivalent classes in the linear path space. Next we define $|i,\ l,\ u|$ to be a midpoint operation[6] since we need to calculate the midpoint of each key state space partition, which is to be the state index of each scenario node:

$$|i,\ l,\ u| = \begin{cases} (u+l)/2 & \text{if an integer} \\ \min\left[(u+l)/2\right] & \text{if } (u+l)/2 > T(i)/2 \\ \max\left[(u+l)/2\right] & \text{otherwise} \end{cases} \tag{B.1}$$

where i denotes the index of the term segment, u and l denote the upper and lower bound of each key state space partition respectively, $min[x]$ gives the greatest integer less than or equal to x and $max[x]$ the smallest integer greater than or equal to x.

The scenario nodes are defined as the node $n(i,\ J) = (T(i)–1,\ |i,\ l,\ u| = |i,\ J|)$ on the binomial path space in Figure B.2.

Figure B.2. Scenario Node

term segment T(i)	T(i)–1	Scenario Node										
1	0						0					
12	11					2	6	9				
36	35				6	14	18	21	29			
60	59			6	18	26	30	33	41	53		
84	83		6	18	30	38	42	45	53	65	77	
120	119	9	24	36	48	56	60	63	71	83	95	110

Three scenario nodes of (11, 2), (11, 6), (11, 9) in the first term segment, are calculated by applying the midpoint operation to the first three key state space partition (0, 3), (4, 7), (8, 11) respectively. The scenario node (11, 2) is calculated by (T(1)−1, max[(0+3)/2]), the scenario node (11, 6) by (T(1)–1, max[(4+7)/2]) and the scenario node (11, 9) by (T(1)–1, min[(8+11)/2]).

A branch, $b(i, J, K)$ is the shortest interest rate path that links the node $(i-1, J)$ to the node (i, K). The branch is defined as for each j, $T(i-1)-1 < j < T(i)-1$, $y = |i-1, J| + (|i, K| - |i-1, J|) \times \{j - (T(i-1) - 1)\} / [T(i) - T(i-1)]$. Then the state corresponding to the j^{th} month is the integer of y. The branches that connect the segments represent the representative path of the equivalent class. Figure B.3 shows the branch geometrically, which is the hypotenuse of a right triangle.

[6] Note that the midpoint operation is slightly different from Ho (1992). We move all the scenario nodes, outside the center segment, one step toward the center segment. The midpoint operation can be defined in a different manner according to each model considered under condition that it should be systematic.

Figure B.3. Branch $b(i, J, K)$

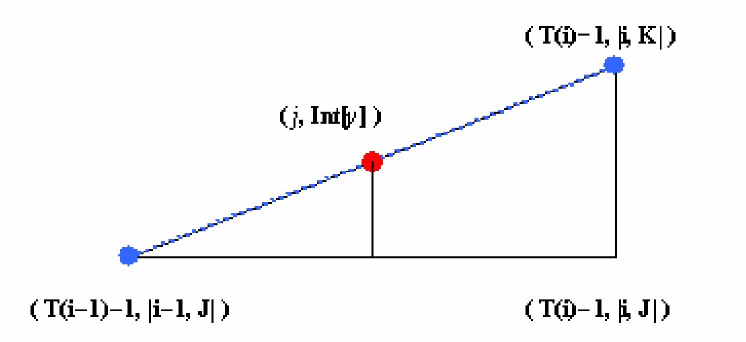

$$\boldsymbol{T(i) - T(i-1) : |i, K| - |i, J| = j - (T(i-1) - 1) : y - |i, J|}$$

We now present how to calculate each representative path probability of LPS model. Consider a representative path, which passes through the scenario node (0, 0), (11, 9) and (35, 21) in Figure B.4. There are 3^2 equivalent classes and the area, through which this representative path passes, represents one of nine equivalent classes. The probability of each representative path is the ratio of the number of paths in the equivalent class, where each representative path belongs, to the total number of paths. The total number of paths is 2^{35} and the number of paths in the equivalent class considered can be calculated by the sum of all the elements in the one-by-four matrix resulting from the following matrix multiplication in Equation (B.2):

Figure B.4. Representative Paths and Their Probabilities

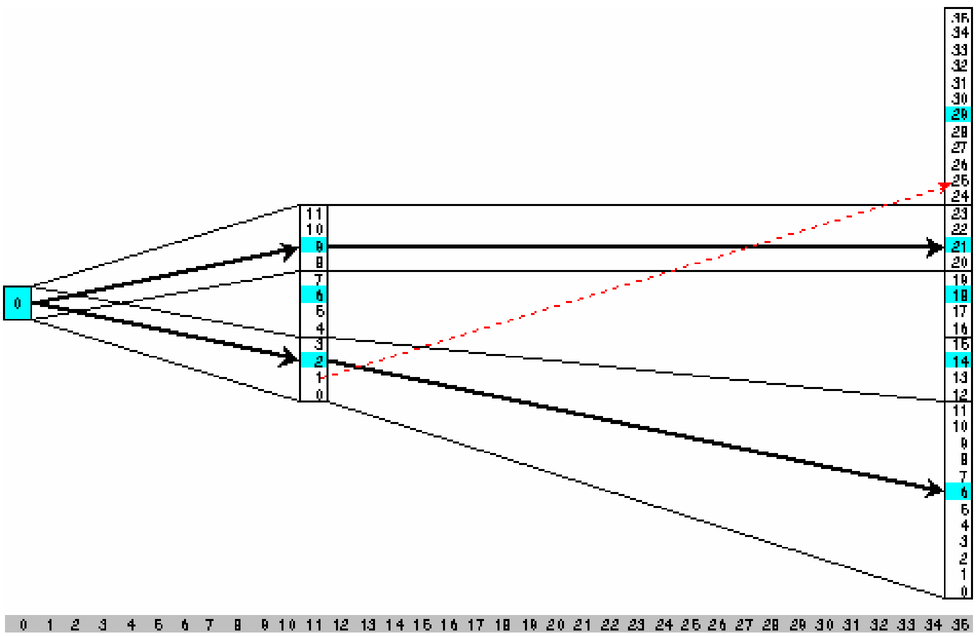

$$\begin{bmatrix} {}_{11}C_8 & {}_{11}C_9 & {}_{11}C_{10} & {}_{11}C_{11} \end{bmatrix} \cdot \begin{bmatrix} {}_{24}C_{20-8} & {}_{24}C_{21-8} & {}_{24}C_{22-8} & {}_{24}C_{23-8} \\ {}_{24}C_{20-9} & {}_{24}C_{21-9} & {}_{24}C_{22-9} & {}_{24}C_{23-9} \\ {}_{24}C_{20-10} & {}_{24}C_{21-10} & {}_{24}C_{22-10} & {}_{24}C_{23-10} \\ {}_{24}C_{20-11} & {}_{24}C_{21-11} & {}_{24}C_{22-11} & {}_{24}C_{23-11} \end{bmatrix} \tag{B.2}$$

The first matrix, which is a row vector, in Equation (B.2) represents the number of paths going from the initial node to the four nodes in the key state space partition (8, 11) at time 11. The second matrix in Equation (B.2) represents the number of paths going from the four nodes in the key state space partition (8, 11) at time 11 to the four nodes in the key state space partition (20, 23) at time 35.

The first column of the one-by-four matrix resulting from Equation (B.2) represents the sum of the number of path going from the initial node via all the nodes in the key state space partition (8, 11) at time 11 to the node (35, 20). The second column of the one-by-four matrix resulting from Equation (B.2) represents the sum of the number of path going from the initial node via all the nodes in the key state space partition (8, 11) at time 11 to the node (35, 21). The third and the fourth column can be interpreted in a similar way with the last node being (35, 22) and (35, 23) respectively. The sum of all the elements in the one-by-four matrix resulting from Equation (B.2) is the total number of paths going from the initial node via all the nodes in the key state space partition (8, 11) at the first segment to all the nodes in the key state space partition (20, 23) at the second segment. Dividing this sum by 2^{35} gives the probability of this representative path passing through the scenario node (0, 0), (11, 9) and (35, 21).

The remaining eight path probabilities can be calculated in similar ways. Consider the representative path going through the scenario node (0, 0), (11, 2), and (35, 6) in Figure B.4. The total number of paths going from the initial node via four nodes in the key state space partition (0, 3) at time 11 to the 12 nodes in the key state space partition (0, 11) at time 35 is calculated by the sum of all the elements in the one-by-twelve matrix resulting from the following matrix multiplication:

$$\begin{bmatrix} {}_{11}C_0 & {}_{11}C_1 & {}_{11}C_2 & {}_{11}C_3 \end{bmatrix} \cdot \begin{bmatrix} {}_{24}C_{0-0} & {}_{24}C_{1-0} & \cdots & {}_{24}C_{10-0} & {}_{24}C_{11-0} \\ {}_{24}C_{0-1} & {}_{24}C_{1-1} & \cdots & {}_{24}C_{10-1} & {}_{24}C_{11-1} \\ {}_{24}C_{0-2} & {}_{24}C_{1-2} & \cdots & {}_{24}C_{10-2} & {}_{24}C_{11-2} \\ {}_{24}C_{0-3} & {}_{24}C_{1-3} & \cdots & {}_{24}C_{10-3} & {}_{24}C_{11-3} \end{bmatrix} \tag{B.3}$$

Dividing Equation (B.3) by the total number of paths of 2^{35} gives the probability of representative path considered. More generally, the probability of the representative path, starting at initial node through the scenario node within a key sate space partition (i, j) at time n arriving at the scenario node within a key state partition (ii, jj) at time nn, is calculated by the sum of all the elements in the 1-by-$(jj-ii+1)$ matrix resulting from the following matrix multiplication:

$$\frac{1}{2^{nn}}\begin{bmatrix} {}_nC_i & {}_nC_{i+1} & \cdots & {}_nC_{j-1} & {}_nC_j \end{bmatrix}\cdot\begin{bmatrix} {}_{nn-n}C_{ii-i} & {}_{nn-n}C_{(ii+1)-i} & \cdots & {}_{nn-n}C_{jj-i} \\ {}_{nn-n}C_{ii-(i+1)} & \ddots & \ddots & \vdots \\ \vdots & \ddots & \ddots & {}_{nn-n}C_{jj-(j-1)} \\ {}_{nn-n}C_{ii-j} & \cdots & {}_{nn-n}C_{(jj-1)-j} & {}_{nn-n}C_{jj-j} \end{bmatrix} \tag{B.4}$$

where ${}_nC_i = 0$ when $n < 0$ or $i < 0$ or $i > n$ by definition. Equation (B.4) can be generalized for any number of term segments with the number of matrices being equal to that of the term segments.

But the sum of nine path probabilities is not equal to unity since such a path going through node (11, 1) and node (35, 25) in Figure B.4 is not included in the equivalent classes of LPS model. So we have to normalize each representative path probability with the sum of nine representative path probabilities in order to make the sum of nine normalized representative path probabilities equal unity according to the law of total probabilities.

Figure B.5 shows the 243 (=3^5) representative path probabilities when we use five segments of (0, 11), (12, 35), …, (84, 119). They are symmetric and the sum of them equals unity. The maximum value is 0.065 and the minimum is 1.39×10^{-16}.

Figure B.5. Representative Path Probability of LPS Model

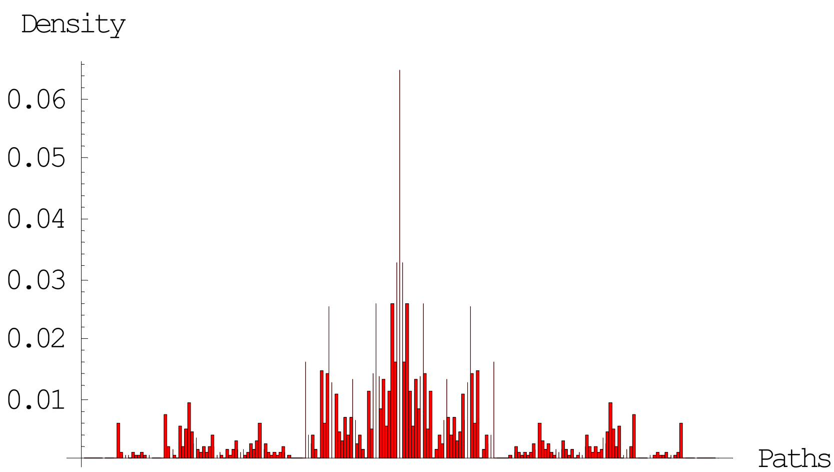

Appendix C: Historical estimates of correlation coefficients between stock index and the first two principal components of yield curve dynamics

Define $\Delta R_{t,j} = R_{t,j} - R_{t-1,j}$ to be the increment of ISDA mid-market par swap rates[7] for all maturity j = {1, 2, 3, 4, 5, 7, 10, 30} at each time t. The dimension of the data matrix is 59×8.

Let **X** be the normalized data matrix such that each column in 59×8 data matrix has mean 0 and variance 1 by subtracting the sample mean and divided by the sample standard deviation such that the first principal component will not be dominated by the input variables with the greatest volatility.

$$\mathbf{X} = \frac{\Delta R_{t,j} - \overline{\Delta R_{\bullet,j}}}{\sigma_{\Delta R_{\bullet,j}}}$$

Let $\underset{(8\times 8)}{\mathbf{V}} = \frac{\mathbf{X}'\mathbf{X}}{T}$ be the correlation matrix between the variables in **X** where T = 59-1.

V =

$$\begin{pmatrix}
1. & 0.917518 & 0.82458 & 0.759817 & 0.71393 & 0.654843 & 0.595615 & 0.490347 \\
0.917518 & 1. & 0.976803 & 0.943265 & 0.913835 & 0.873442 & 0.830175 & 0.735833 \\
0.82458 & 0.976803 & 1. & 0.991824 & 0.97761 & 0.953004 & 0.921989 & 0.841727 \\
0.759817 & 0.943265 & 0.991824 & 1. & 0.996071 & 0.982378 & 0.959842 & 0.891065 \\
0.71393 & 0.913835 & 0.97761 & 0.996071 & 1. & 0.994209 & 0.978011 & 0.918426 \\
0.654843 & 0.873442 & 0.953004 & 0.982378 & 0.994209 & 1. & 0.993953 & 0.951512 \\
0.595615 & 0.830175 & 0.921989 & 0.959842 & 0.978011 & 0.993953 & 1. & 0.976985 \\
0.490347 & 0.735833 & 0.841727 & 0.891065 & 0.918426 & 0.951512 & 0.976985 & 1.
\end{pmatrix}$$

Let **W** be the 8×8 matrix of eigenvectors of **V**, ordered according to the size of corresponding eigenvalues such that $\lambda_1 > \lambda_2 > ... > \lambda_m$. Thus **VW**=**WΛ** where **Λ** is the 8×8 matrix of eigenvalues of **V**. Then the mth column of **W**, denoted $\mathbf{w}_m = (w_{1m}, ..., w_{8m})'$, is the 8×1 eigenvector corresponding to the eigenvalue λ_m.

W =

$$\begin{pmatrix}
-0.290893 & 0.711042 & 0.518715 & -0.354952 & -0.081126 & -0.0842736 & -0.0263692 & 0.0191104 \\
-0.353773 & 0.357982 & -0.138602 & 0.60152 & 0.420917 & 0.352951 & 0.182013 & -0.17545 \\
-0.369521 & 0.126045 & -0.313572 & 0.298796 & -0.223419 & -0.384954 & -0.398744 & 0.550326 \\
-0.371919 & -0.0110639 & -0.313634 & -0.0583506 & -0.414941 & -0.274344 & 0.0566458 & -0.713536 \\
-0.370679 & -0.100227 & -0.258929 & -0.327525 & -0.224637 & 0.333661 & 0.606278 & 0.385836 \\
-0.366669 & -0.20864 & -0.0938812 & -0.373201 & 0.207977 & 0.476165 & -0.629464 & -0.087854 \\
-0.359726 & -0.30601 & 0.112458 & -0.18362 & 0.630633 & -0.540936 & 0.200143 & 0.0149709 \\
-0.337793 & -0.4506 & 0.65309 & 0.373136 & -0.320531 & 0.119141 & 0.0107442 & 0.00692073
\end{pmatrix}$$

[7] Sample period is 2000/08 - 2005/07 from http://www.federalreserve.gov/releases/h15/data.htm.

$\mathbf{\Lambda} =$

$$\begin{pmatrix} 7.17589 & 0 & 0 & 0 & 0 & 0 & 0 & 0 \\ 0 & 0.736424 & 0 & 0 & 0 & 0 & 0 & 0 \\ 0 & 0 & 0.0685601 & 0 & 0 & 0 & 0 & 0 \\ 0 & 0 & 0 & 0.015835 & 0 & 0 & 0 & 0 \\ 0 & 0 & 0 & 0 & 0.00213678 & 0 & 0 & 0 \\ 0 & 0 & 0 & 0 & 0 & 0.000666959 & 0 & 0 \\ 0 & 0 & 0 & 0 & 0 & 0 & 0.000297403 & 0 \\ 0 & 0 & 0 & 0 & 0 & 0 & 0 & 0.000186879 \end{pmatrix}$$

Figure C.1. The plot of the first three eigenvectors

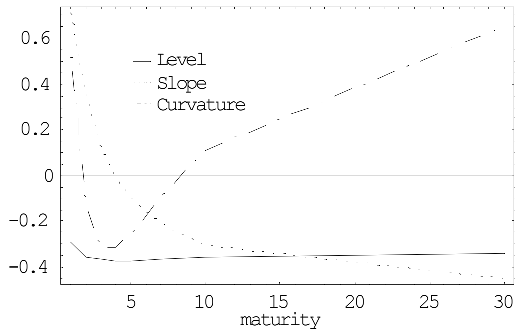

The first three eigenvalues corresponding to those eigenvectors are $\{\lambda_1, \lambda_2, \lambda_3\}$ = {7.17589, 0.736424, 0.0685601} and their cumulative weight are {0.896987, 0.98904, 0.99761} respectively.

Define the *m*th principal component of the system by

$$\mathbf{p}_m = \begin{bmatrix} p_{1,m} \\ p_{2,m} \\ \vdots \\ p_{59,m} \end{bmatrix} = w_{1,m} \begin{bmatrix} x_{1,1} \\ x_{2,1} \\ \vdots \\ x_{59,1} \end{bmatrix} + w_{2,m} \begin{bmatrix} x_{1,2} \\ x_{2,2} \\ \vdots \\ x_{59,2} \end{bmatrix} + \ldots + w_{8,m} \begin{bmatrix} x_{1,8} \\ x_{2,8} \\ \vdots \\ x_{59,8} \end{bmatrix} = w_{1m}\mathbf{x}_1 + w_{2m}\mathbf{x}_2 + \ldots + w_{8m}\mathbf{x}_8$$
$$= \mathbf{X}\mathbf{w}_m$$

where $\mathbf{x}_i$ denotes the ith column of $\mathbf{X}$, i.e., the standardized historical input data on the ith variable in the system.

Each principal component is a time series of the transformed $\mathbf{X}$ variables, and the full 59×8 matrix of principal components, which has $\mathbf{p}_m$ as its *m*th column, may be written

$$\mathbf{P} = \mathbf{X}\mathbf{W}. \tag{C.1}$$

To see that this procedure leads to uncorrelated components, note that

$\mathbf{P}'\mathbf{P} = \mathbf{W}'\mathbf{X}'\mathbf{X}\mathbf{W} = T\mathbf{W}'\mathbf{W}\mathbf{\Lambda}$.

However, $\mathbf{W}$ is an orthogonal matrix, that is $\mathbf{W}' = \mathbf{W}^{-1}$ and so $\mathbf{P}'\mathbf{P} = T\mathbf{\Lambda}$. Since this is a diagonal matrix the columns of $\mathbf{P}$ are uncorrelated, and the variance of the *m*th principal component is λ_m.

Since the variance of each principal component is determined by its corresponding eigenvalues, the proportion of the total variation in X that is explained by the *m*th principal component is $\lambda_m \Big/ \sum_{i=1}^{8} \lambda_i$. However, the sum of the eigenvalues is 8, the number of variables in the system.[8] Therefore the proportion of variation explained by the first *n* principal component together is

$$\sum_{i=1}^{n} \lambda_i \Big/ 8 .$$

Because of the choice of column labeling in $\mathbf{W}$ the principal components have been ordered so that $\mathbf{p}_1$ belongs to the first and largest eigenvalue λ_1, $\mathbf{p}_2$ belongs to the second largest eigenvalue λ_2, and so on. In a highly correlated system the first eigenvalue will be much larger than the others, so the first principal component alone will explain a large part of the variation.

Since $\mathbf{W}' = \mathbf{W}^{-1}$, Equation (C.1) is equivalent to $\mathbf{X} = \mathbf{P}\mathbf{W}'$, that is,

$$\mathbf{x}_i = \begin{bmatrix} x_{1,i} \\ x_{2,i} \\ \vdots \\ x_{59,i} \end{bmatrix} = w_{i,1} \begin{bmatrix} p_{1,1} \\ p_{2,1} \\ \vdots \\ p_{59,1} \end{bmatrix} + w_{i,2} \begin{bmatrix} p_{1,2} \\ p_{2,2} \\ \vdots \\ p_{59,2} \end{bmatrix} + \ldots + w_{i,8} \begin{bmatrix} p_{1,8} \\ p_{2,8} \\ \vdots \\ p_{59,8} \end{bmatrix} = w_{i,1}\mathbf{p}_1 + w_{i,2}\mathbf{p}_2 + \ldots + w_{i,8}\mathbf{p}_8 \qquad \text{(C.2)}$$

Thus each vector of input data may be written as a linear combination of the principal components. This is the principal components representation of the original variables that lies at the core of PCA models. Often only the first few principal components are used to represent each of the input variables, because they are sufficient to explain most of the variation in the system.

$$\mathbf{x}_i = w_{i,1}\mathbf{p}_1 + w_{i,2}\mathbf{p}_2 + w_{i,3}\mathbf{p}_3$$

That is, we can approximate the original stationary data matrix

[8] To see why, note that the sum of the eigenvalues is the trace of $\mathbf{\Lambda}$, the diagonal matrix of eigenvalues of $\mathbf{V}$. However, the trace of $\mathbf{\Lambda}$ equals the trace of $\mathbf{V}$ (because trace is invariant under similarity transformation), and because $\mathbf{V}$ has 1s all along its diagonal, the trace of $\mathbf{V}$ is the number of variables in the system.

$$\underset{(59\times8)}{\mathbf{X}} = \mathbf{PW}' = \underset{(59\times8)}{\begin{bmatrix} p_{1,1} & p_{1,2} & \cdots & p_{1,8} \\ p_{2,1} & p_{2,2} & \cdots & p_{2,8} \\ \vdots & \vdots & \ddots & \vdots \\ p_{59,1} & p_{59,2} & \cdots & p_{59,8} \end{bmatrix}} \underset{(8\times8)}{\begin{bmatrix} w_{1,1} & w_{2,1} & \cdots & w_{8,1} \\ w_{1,2} & w_{2,2} & \cdots & w_{8,2} \\ \vdots & \vdots & \ddots & \vdots \\ w_{1,8} & w_{2,8} & \cdots & w_{8,8} \end{bmatrix}}$$

with

$$\underset{(59\times8)}{\mathbf{X}} \cong \underset{(59\times3)}{\begin{bmatrix} p_{1,1} & p_{1,2} & p_{1,3} \\ p_{2,1} & p_{2,2} & p_{2,3} \\ \vdots & \vdots & \vdots \\ p_{59,1} & p_{59,2} & p_{59,3} \end{bmatrix}} \underset{(3\times8)}{\begin{bmatrix} w_{1,1} & w_{2,1} & \cdots & w_{8,1} \\ w_{1,2} & w_{2,2} & \cdots & w_{8,2} \\ w_{1,3} & w_{2,3} & \cdots & w_{8,3} \end{bmatrix}}.$$

Finally, the historical estimates of correlation coefficients between stock index and the first two principal components of yield curve dynamics can be calculated by $\rho_1 = corr(\mathbf{dS}/\mathbf{S}, \mathbf{P}_1) = -0.287435$ and $\rho_2 = corr(\mathbf{dS}/\mathbf{S}, \mathbf{P}_2) = 0.0322811$.

Figure C.2. The scattered plot of index return and principal component

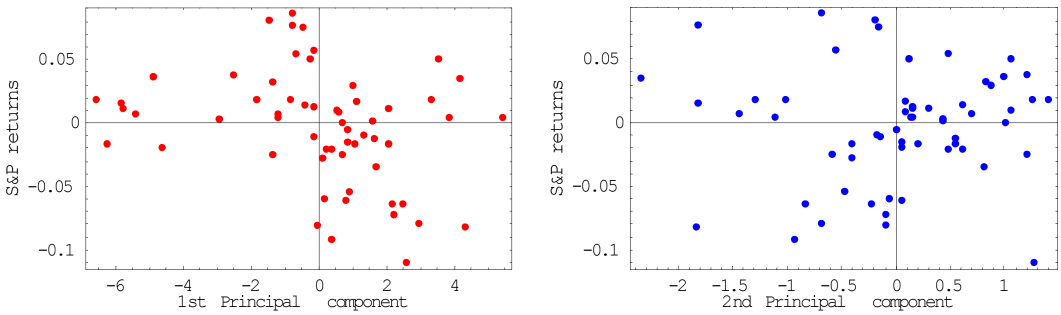

Appendix D: Cholesky decomposition

Consider the situation where we require n correlated samples from normal distributions with the correlation between sample i and sample j being ρ_{ij}. We first sample n *independent* variables x_i $(1 \le i \le n)$, from univariate standardized normal distributions. The required samples, ε_i $(1 \le i \le n)$, are then defined as follows:

$$\varepsilon_1 = \alpha_{11} x_1$$
$$\varepsilon_2 = \alpha_{21} x_1 + \alpha_{22} x_2$$
$$\varepsilon_3 = \alpha_{31} x_1 + \alpha_{32} x_2 + \alpha_{33} x_3$$

and so on. We choose the coefficients α_{ij} so that the correlations and variances are correct. This can be done step by step as follows. Set $\alpha_{11} = 1$; choose α_{21} so that $\alpha_{21}\alpha_{11} = \rho_{21}$, choose α_{22} so that $\alpha_{21}^2 + \alpha_{22}^2 = 1$; choose α_{31} so that $\alpha_{31}\alpha_{11} = \rho_{31}$; choose α_{32} so that $\alpha_{31}\alpha_{21} + \alpha_{32}\alpha_{22} = \rho_{32}$; choose α_{33} so that $\alpha_{31}^2 + \alpha_{32}^2 + \alpha_{33}^2 = 1$; and so on. In summary, $\varepsilon_i = \sum_{k=1}^{i} \alpha_{ik} x_k$, $\sum_{k=1}^{i} \alpha_{ik}^2 = 1$, $\sum_{k=1}^{j} \alpha_{ik}\alpha_{jk} = \rho_{ij} (j < i)$. This procedure is known as the *Cholesky decomposition*.

Then

$$\alpha_{11} = 1,$$
$$\alpha_{21} = \rho_{21},\ \alpha_{22} = \sqrt{1-\rho_{21}^2},$$
$$\alpha_{31} = \rho_{31},\ \alpha_{32} = \frac{\rho_{32} - \rho_{31}\rho_{21}}{\sqrt{1-\rho_{21}^2}}, \quad \alpha_{33} = \sqrt{1-\alpha_{31}^2-\alpha_{32}^2} = \frac{\sqrt{1-\rho_{21}^2-\rho_{31}^2-\rho_{32}^2+2\rho_{31}\rho_{32}\rho_{21}}}{\sqrt{1-\rho_{21}^2}}$$

Example 1: The two-factor Gaussian interest rate model (G2++) and the equity fund value S_t (Chu and Kwok)

For the G2++ model, the interest rate r_t is given by

$$r_t = b(t) + x_{1,t} + x_{2,t}$$

where the dynamics of the risk factors are governed by

$$dx_1 = -k_1 x_1 dt + \sigma_1 dZ_1 \tag{D.1}$$
$$dx_2 = -k_2 x_2 dt + \sigma_2 \left(\rho dZ_1 + \sqrt{1-\rho^2}\, dZ_2\right) \tag{D.2}$$

Here, $b(t)$ is a function which is determined by fitting the current interest rate term structure and ρ is the correlation coefficient between the risk factors. And the dynamics of the equity fund value is given by

$$\frac{dS_t}{S_t} = (r-q)dt + \sigma_S \left(\rho_{S1} dZ_1 + \rho_{S2} dZ_2 + \sqrt{1-\rho_{S1}^2 - \rho_{S2}^2}\, dZ_3 \right) \tag{D.3}$$

where the correlations of equity fund value and the risk factors of interest rate are ρ_{S1} and ρ_{S2} respectively. We can see that Equation (D.1), (D.2), and (D.3) are the direct application of the *Cholesky* decomposition except that the standard deviations of the correlated random variables are σ_1, σ_1, and σ_S respectively not unity.

Proof

We have only to check that the value of α_{ij}.
It can be easily checked that

$$\alpha_{11} = 1,$$

$$\alpha_{21} = \rho_{21} = \rho, \quad \alpha_{22} = \sqrt{1-\rho_{21}^2} = \sqrt{1-\rho^2},$$

$$\alpha_{31} = \rho_{31} = \rho_{S1},$$

$$\alpha_{32} = \frac{\rho_{32} - \rho_{31}\rho_{21}}{\sqrt{1-\rho_{21}^2}} = \frac{\left(\rho_{S1}\rho + \rho_{S2}\sqrt{1-\rho^2}\right) - \rho_{S1}\rho}{\sqrt{1-\rho^2}} = \rho_{S2}$$

$$\because \rho_{32} = corr\left(\frac{dS}{S}, dx_2\right) = \frac{\sigma_2 \rho \sigma_S \rho_{S1} dt + \sigma_2 \sqrt{1-\rho^2}\, \sigma_S \rho_{S2} dt}{\sigma_2 \sqrt{dt} \cdot \sigma_S \sqrt{dt}} = \rho_{S1}\rho + \rho_{S2}\sqrt{1-\rho^2}$$

$$\begin{aligned}
\alpha_{33} &= \frac{\sqrt{1-\rho_{21}^2 - \rho_{31}^2 - \rho_{32}^2 + 2\rho_{31}\rho_{32}\rho_{21}}}{\sqrt{1-\rho_{21}^2}} \\
&= \frac{\sqrt{1-\rho^2-\rho_{S1}^2 - \left(\rho_{S1}\rho + \rho_{S2}\sqrt{1-\rho^2}\right)^2 + 2\rho_{S1}\left(\rho_{S1}\rho + \rho_{S2}\sqrt{1-\rho^2}\right)\rho}}{\sqrt{1-\rho^2}} \\
&= \frac{\sqrt{\left(1-\rho^2\right)\left(1-\rho_{S1}^2 - \rho_{S2}^2\right)}}{\sqrt{1-\rho^2}} = \sqrt{1-\rho_{S1}^2 - \rho_{S2}^2}
\end{aligned}$$

Therefore, we have proved that Equation (D.3) is the direct application of Cholesky decomposition where dZ_1, dZ_2, and dZ_3 are the *independent* standard Wiener process respectively and $\alpha_{31} = \rho_{S1}$, $\alpha_{32} = \rho_{S2}$, and $\alpha_{33} = \sqrt{1-\rho_{S1}^2 - \rho_{S2}^2}$

Q.E.D.

Example 2: The two-factor generalized Ho-Lee model and the account value V (Ho, Lee, and Choi)

The short rate process under two-factor generalized Ho-Lee model is given by

$$\mathrm{d}r = \theta(r, t)\mathrm{d}t + \sigma_{r1}(r, t)\mathrm{d}W_1 + \sigma_{r2}(r, t)\mathrm{d}W_2 \tag{D.4}$$

GHL assumes that the two factors are independent, that is ρ in Equation (D.2) is zero. $\theta(r, t)$ depends on the initial spot yield curve and the term structure of volatilities. $\sigma_{r1}(r, t)$ and $\sigma_{r2}(r, t)$ are the term structure volatilities of the interest rate model. Each of the volatilities has the behavior that

$$\sigma_{ri}(r,t) = \begin{cases} \sigma_i(t)R & when\ r > R \\ \sigma_i(t)r & when\ r < R \end{cases}$$

The account value process is given by as follows:

$$\frac{\mathrm{d}V}{V} = (r-f)\mathrm{d}t + \sigma\left(\rho_1 \mathrm{d}W_1 + \rho_2 \mathrm{d}W_2 + \sqrt{1-\rho_1^2-\rho_2^2}\,\mathrm{d}Z\right) \tag{D.5}$$

where the correlations of account value and the risk factors of interest rate are ρ_1 and ρ_2 respectively. We can also see that Equation (D.5) is the direct application of the *Cholesky* decomposition.

Proof

We have only to check that the value of α_{ij}.
It can be easily checked that

$$\alpha_{11} = 1,$$
$$\alpha_{21} = \rho_{21} = 0, \quad \alpha_{22} = \sqrt{1-\rho_{21}^2} = 1,$$
$$\alpha_{31} = \rho_{31} = \rho_1,$$
$$\alpha_{32} = \frac{\rho_{32} - \rho_{31}\rho_{21}}{\sqrt{1-\rho_{21}^2}} = \frac{\rho_2 - \rho_1 \cdot 0}{\sqrt{1-0^2}} = \rho_2$$
$$\because \rho_{32} = corr\left(\frac{dV}{V}, \sigma_{r2}(r,t)dW_2\right) = \frac{\sigma\rho_2\sigma_{r2}(r,t)dt}{\sigma\sqrt{dt}\cdot\sigma_{r2}(r,t)\sqrt{dt}} = \rho_2$$

$$\alpha_{33} = \frac{\sqrt{1-\rho_{21}^2-\rho_{31}^2-\rho_{32}^2+2\rho_{31}\rho_{32}\rho_{21}}}{\sqrt{1-\rho_{21}^2}} = \frac{\sqrt{1-0^2-\rho_1^2-\rho_2^2+2\rho_1\rho_2\cdot 0}}{\sqrt{1-0^2}}$$
$$= \sqrt{1-\rho_1^2-\rho_2^2}$$

Therefore, we have proved that Equation (D.5) is the direct application of Cholesky decomposition where dW_1, dW_2, and dZ are the *independent* standard Wiener process respectively.

Appendix E. The local conditional distribution of the account value process given two-factor LPS model

Now we calculate the local conditional distribution, e.g., expected value and variance, of the account value process.

The expected value is given by as follows:

$$
\begin{aligned}
&E\left[V(n+\Delta t) \mid r(n;i,j), \varepsilon_1, \varepsilon_2\right] \\
&= V(n;i,j) E\left[e^X\right] \\
&\textit{where } X \sim N\left(\left(r(n;i,j) - f - \sigma^2/2\right)\Delta t + \sigma\left(\rho_1\varepsilon_1 + \rho_2\varepsilon_2\right)\sqrt{\Delta t},\ \ \sigma\sqrt{1-\rho_1^2-\rho_2^2}\sqrt{\Delta t}\right) \\
&= V(n;i,j)\exp\left\{\left(r(n;i,j) - f\right)\Delta t + \sigma\left(\rho_1\varepsilon_1 + \rho_2\varepsilon_2\right)\sqrt{\Delta t} - \frac{1}{2}\sigma^2\left(\rho_1^2+\rho_2^2\right)\Delta t\right\}
\end{aligned}
$$

where we have used the fact that

$$
\begin{aligned}
&E\left[e^{\theta X}\right] = \exp\left\{\mu\theta + \frac{1}{2}\sigma^2\theta^2\right\} \\
&\text{when } X \sim N\left(\mu,\ \sigma\right)
\end{aligned}
$$

The combination of the values that ε_1 and ε_2 can have is {{1,1}, {1,-1}, {-1,1},{-1,-1}} and we already know the information of the values from the LPS lattice.

The variance is given by as follows:

$$
\begin{aligned}
&\operatorname{var}\left[V(n+\Delta t) \mid r(n;i,j), \varepsilon_1, \varepsilon_2\right] \\
&= E\left[V(n)^2 e^{2X}\right] - \left(E\left[V(n)e^X\right]\right)^2 \\
&= V(n)^2 \exp\left\{2\left(r(n;i,j) - f\right)\Delta t + 2\sigma\left(\rho_1\varepsilon_1 + \rho_2\varepsilon_2\right)\sqrt{\Delta t} - \sigma^2\left(\rho_1^2+\rho_2^2\right)\Delta t\right\}\left(e^{\sigma^2\left(1-\rho_1^2-\rho_2^2\right)\Delta t} - 1\right)
\end{aligned}
$$

Appendix F. Calibration of LPS model

There are two methods of calibrating the LPS model to the initial yield curve. The first method is to calibrate the sum of all the weighted pathwise values of LPS model to the initial yield curve. This method preserves the volatility and recombining structure of the representative paths after calibration.

Example 1. Calibration to initial term structure such that the sum of all the weighted pathwise values of LPS model equals the initial yield curve

Consider pricing one-year zero-coupon bond using the LPS model with one term segment at time 11. The following sets of indices represent the nodes that three representative paths follow in the linear path space.

{{{0,0},{1,0},{2,0},{3,0},{4,0},{5,0},{6,1},{7,1},{8,1},{9,1},{10,1},{11,2}},
{{0,0},{1,0},{2,1},{3,1},{4,2},{5,2},{6,3},{7,3},{8,4},{9,4},{10,5},{11,6}},
{{0,0},{1,0},{2,1},{3,2},{4,3},{5,4},{6,4},{7,5},{8,6},{9,7},{10,8},{11,9}}}

The node $\{n, i\}$ represents time n and state i in monthly step size. The first and the last nodes in each path are the scenario nodes and the interim nodes are the branches connecting these scenario nodes.
The representative path probabilities are $\{Q_1, Q_2, Q_3\}$, calculated using the algorithm in Appendix B. The first calibration scheme is to find the unknown x_0, which satisfies the following equation:

$$p(1) = Q_1 \exp\left\{-\left(r_0^0(1) + x_0\right)\right\} + Q_2 \exp\left\{-\left(r_0^0(1) + x_0\right)\right\} + Q_3 \exp\left\{-\left(r_0^0(1) + x_0\right)\right\}$$

where $p(1)$ is the initial one-period discount function in monthly step size and $r_0^0(1)$ is the one period interest rate at time 0 and state 0. Of course, the optimal solution for x_0 at initial time is zero for the obvious reason. The next step is to find the unknown x_1, which satisfies the following equation:

$$\begin{aligned} p[2] = {} & Q1\exp\left\{-\left(r_0^0(1) + x_0^* + r_0^1(1) + x_1\right)\right\} + Q2\exp\left\{-\left(r_0^0(1) + x_0^* + r_0^1(1) + x_1\right)\right\} \\ & + Q3\exp\left\{-\left(r_0^0(1) + x_0^* + r_0^1(1) + x_1\right)\right\} \end{aligned}.$$

We repeat this procedure 10 times more up to $p[12]$ in order to find the remaining unknowns $x_2, \ldots, x_{11}$.

$$\begin{aligned} p[12] = {} & Q1\exp\left\{-\left(r_0^0(1) + x_0^* + r_0^1(1) + x_1^* + r_0^2(1) + x_2^* + \cdots + r_1^{10}(1) + x_{10}^* + r_2^{11}(1) + x_{11}\right)\right\} \\ & + Q2\exp\left\{-\left(r_0^0(1) + x_0^* + r_0^1(1) + x_1^* + r_1^2(1) + x_2^* + \cdots + r_5^{10}(1) + x_{10}^* + r_6^{11}(1) + x_{11}\right)\right\} \\ & + Q3\exp\left\{-\left(r_0^0(1) + x_0^* + r_0^1(1) + x_1^* + r_1^2(1) + x_2^* + \cdots + r_8^{10}(1) + x_{10}^* + r_9^{11}(1) + x_{11}\right)\right\} \end{aligned}$$

The second method is to calibrate in a state price consistent manner such that the sum of the weighted pathwise values in a certain key state space partition of the LPS model is equal to the sum of the state prices in the same key state space partition of binomial tree, which is useful for the option pricing. For example, consider the key state space partition (20, 23) at time 35 in Figure F.1.

Figure F.1. Three-Year Zero-Coupon Bond and Caplet Price of LPS Model with Two Term Segments

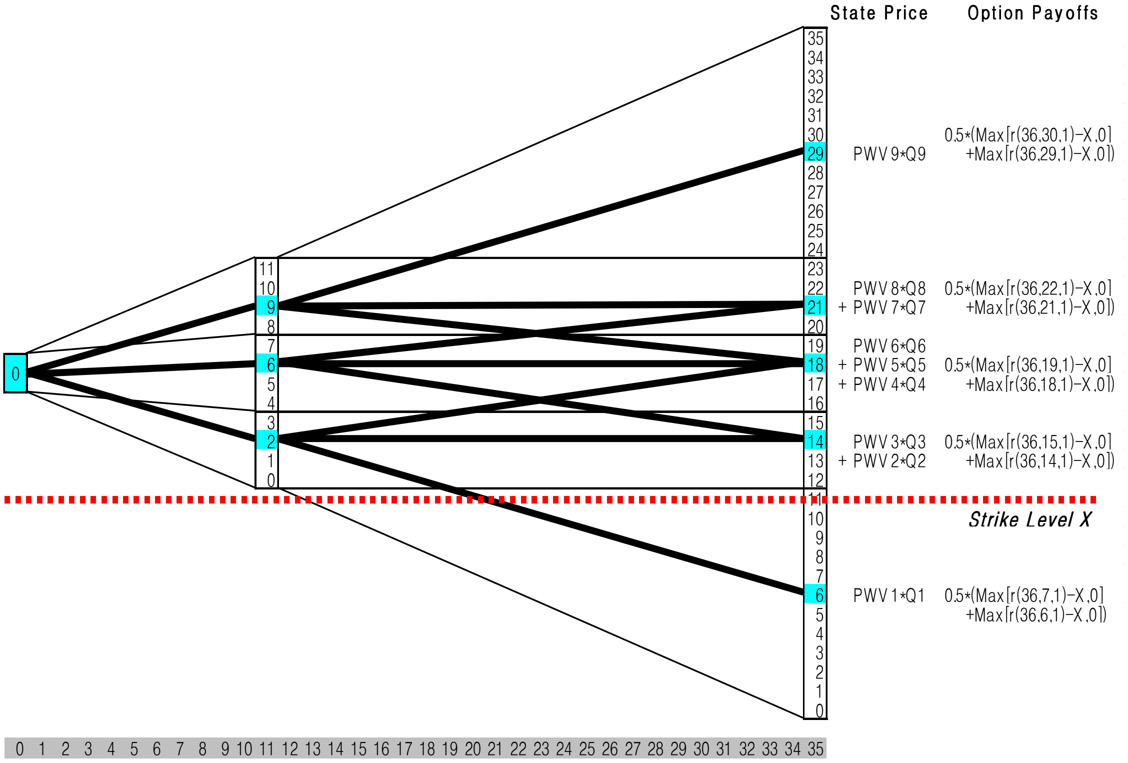

We calibrate the sum of two weighted pathwise values to the sum of four Arrow-Debreu securities' prices in the same segment, that is, $PWV_7 \times Q_7 + PWV_8 \times Q_8 = AD(20) + AD(21) + AD(22) + AD(23)$. The correct option value in that segment of the binomial tree is calculated as $AD(20) \cdot C(20) + \cdots + AD(23) \cdot C(23)$ and if the calibration error is negligible the correct option value can be rewritten as $(PWV_7 \times Q_7 + PWV_8 \times Q_8) \times \bar{C}$, where $\bar{C}$, the average option payoffs, is calculated by

$$\bar{C} = \frac{AD(20)}{AD(20) + \cdots + AD(23)} \cdot C(20) + \cdots + \frac{AD(23)}{AD(20) + \cdots + AD(23)} \cdot C(23) \qquad \text{(F.1)}$$

Each option payoff, $C(i)$, in state i is weighted by ratio of the state price, $AD(i)$, in state i to the sum of all the state price in the key state space partition considered. Next we approximate those weights in Equation (F.1) with the binomial coefficients corresponding to each time and state in order to decrease the computational burden and make the LPS model more independent of the binomial tree since these approximate weights are the same as the correct ones in Equation (F.1) when there is no interest rate risk.

$$\bar{C} \cong \frac{{}_{35}C_{20}}{{}_{35}C_{20} + \cdots + {}_{35}C_{23}} \cdot C(20) + \cdots + \frac{{}_{35}C_{23}}{{}_{35}C_{20} + \cdots + {}_{35}C_{23}} \cdot C(23) \tag{F.2}$$

Example 2. Calibration to the initial term structure in a state price consistent manner

Consider pricing the same bond as in Example 1. The second calibration scheme is to find the unknowns "*x*, *y*, and *z*" which minimize the difference between the sum of the weighted pathwise values of LPS model and the sum of state prices in the same key state space partition on the binomial tree as follows:

$$\begin{aligned}
&\left|\left(\sum_{i=0}^{3} AD_i^{11} P_i^{11}(1)\right) - Q_1 \exp\left\{-\left(r_0^0(1) + x + r_0^1(1) + x + r_0^2(1) + x + r_0^3(1) + x + \cdots + r_1^{10}(1) + x + r_2^{11}(1) + x\right)\right\}\right| + \\
&\left|\left(\sum_{i=4}^{7} AD_i^{11} P_i^{11}(1)\right) - Q_2 \exp\left\{-\left(r_0^0(1) + y + r_0^1(1) + y + r_1^2(1) + y + r_1^3(1) + y + \cdots + r_5^{10}(1) + y + r_6^{11}(1) + y\right)\right\}\right| + \\
&\left|\left(\sum_{i=8}^{11} AD_i^{11} P_i^{11}(1)\right) - Q_3 \exp\left\{-\left(r_0^0(1) + z + r_0^1(1) + z + r_1^2(1) + z + r_2^3(1) + z + \cdots + r_8^{10}(1) + z + r_9^{11}(1) + z\right)\right\}\right|
\end{aligned} \tag{F.3}$$

AD_i^n in Equation (F.3) is the Arrow-Debreu security price, which pays \$1 in state *i* at time *n*. $P_i^n(T)$ is a *T*-period discount function in state *i* at time *n*. Under the interest rate uncertainty, the prices of Arrow-Debreu securities, which pay \$1 in each state *i* = {0, 1} at time 1, denoted as AD_i^1, is the (*i*+1)th element of the following (1×2) row vector, *AD*[1]:

$$AD[1] = \begin{bmatrix} \frac{1}{2} P_0^0(1) & \frac{1}{2} P_0^0(1) \end{bmatrix} \tag{F.4}$$

The Arrow-Debreu securities' prices, which pay \$1 in each state *i* = {0, 1, 2} at time 2, denoted as AD_i^2, is the (*i*+1)th element of the following (1×3) row vector, *AD*[2]:

$$AD[2] = \begin{bmatrix} \frac{1}{2} P_0^0(1) & \frac{1}{2} P_0^0(1) \end{bmatrix} \cdot \begin{bmatrix} \frac{1}{2} P_0^1(1) & \frac{1}{2} P_0^1(1) & 0 \\ 0 & \frac{1}{2} P_1^1(1) & \frac{1}{2} P_1^1(1) \end{bmatrix} = AD[1] \cdot \begin{bmatrix} \frac{1}{2} P_0^1(1) & \frac{1}{2} P_0^1(1) & 0 \\ 0 & \frac{1}{2} P_1^1(1) & \frac{1}{2} P_1^1(1) \end{bmatrix} \tag{F.5}$$

Using the recursive relationship as in Equation (F.4) and (F.5) we can easily generate the Arrow-Debreu securities' prices for the arbitrary time horizon. Note that we use

$\sum_{i=0}^{11} AD_i^{11} \cdot P_i^{11}(1)$ instead of $\sum_{i=0}^{12} AD_i^{12}$ in order to calculate the one-year zero-coupon bond price since the term segment is located at time 11. It can be easily verified that[9]

$$\sum_{i=0}^{n} AD_i^n = \sum_{i=0}^{n-1} AD_i^{n-1} P_i^{n-1}(1) . \tag{F.6}$$

Also remember that the option payoff, related with the terminal node, say {35, 6} in Figure F.1, is $\left(\max\left[r_7^{36}(1) - X,\ 0\right] + \max\left[r_6^{36}(1) - X,\ 0\right]\right)/2$. Thus the option price can be calculated by

$$\sum_{i=0}^{35} AD_i^{35} P_i^{35}(1)\left(C_{i+1}^{36} + C_i^{36}\right)/2 \tag{F.7}$$

where $C_i^{36} = \max\left(r_i^{36}(1) - 0.04,\ 0\right)$. And the option price obtained using Equation (F.7) is equal to the value by the backward substitution approach on the binomial tree. Also note

[9] Arrow-Debreu security price in state i at time n (≥ 1) is defined as follows:

$$AD_i^n = \begin{cases} \frac{1}{2} AD_{i-1}^{n-1} P_{i-1}^{n-1}(1) & if\ \ i = n \\ \frac{1}{2} AD_i^{n-1} P_i^{n-1}(1) & if\ \ i = 0 \\ \frac{1}{2} AD_{i-1}^{n-1} P_{i-1}^{n-1}(1) + \frac{1}{2} AD_i^{n-1} P_i^{n-1}(1) & otherwise \end{cases} \tag{F.6.1}$$

Therefore,

$$\begin{aligned} \sum_{i=0}^{n} AD_i^n &= AD_0^n + AD_1^n + AD_2^n + \cdots + AD_{n-1}^n + AD_n^n \\ &= \frac{1}{2} AD_0^{n-1} P_0^{n-1}(1) \\ &\quad + \frac{1}{2} AD_0^{n-1} P_0^{n-1}(1) + \frac{1}{2} AD_1^{n-1} P_1^{n-1}(1) \\ &\quad + \cdots \\ &\quad + \frac{1}{2} AD_{n-2}^{n-1} P_{n-2}^{n-1}(1) + \frac{1}{2} AD_{n-1}^{n-1} P_{n-1}^{n-1}(1) \\ &\quad + \frac{1}{2} AD_{n-1}^{n-1} P_{n-1}^{n-1}(1) \\ &= \sum_{i=0}^{n-1} AD_i^{n-1} P_i^{n-1}(1) \end{aligned} \tag{F.6.2}$$

Q.E.D.

that we use Equation (F.7) instead of $\sum_{i=0}^{36} AD_i^{36} \cdot C_i^{36}$ since the term segment is located at time 35. It can be easily verified that[10]

$$\sum_{i=0}^{n} AD_i^n \cdot C_i^n = \sum_{i=0}^{n-1} AD_i^{n-1} P_i^{n-1}(1)\left(C_{i+1}^n + C_i^n\right)/2. \tag{F.8}$$

Since we use the same number of unknowns as the number of representative paths by parallel-shifting the different amount for each representative path in order to minimize the objective function, the volatility structure of the LPS model collapses and the calibrated interest rate paths do not recombine any more. But it does not matter since the pathwise valuation does not need the recombining tree.

If we consider pricing three-year zero bond using two term segments at time 11 and 35 in Figure F.1 then there are "3^2" pathwise values and "2×2+1" key state space partitions. In this case, we have to sort the nine pathwise values according to the state index of the terminal node of each representative path in an ascending order and then group the representative paths, having the same terminal node, in order to calibrate a state price consistent manner. The grouping order follows the trinomial coefficients. For example,

---

[10] From equation (F.6.1) in footnote 7,

$$AD_i^n C_i^n = \begin{cases} \frac{1}{2} AD_{i-1}^{n-1} P_{i-1}^{n-1}(1) C_i^n & \text{if } i = n \\ \frac{1}{2} AD_i^{n-1} P_i^{n-1}(1) C_i^n & \text{if } i = 0 \\ \frac{1}{2} AD_{i-1}^{n-1} P_{i-1}^{n-1}(1) C_i^n + \frac{1}{2} AD_i^{n-1} P_i^{n-1}(1) C_i^n & \text{otherwise} \end{cases} \tag{F.8.1}$$

Therefore,

$$\begin{aligned} \sum_{i=0}^{n} AD_i^n C_i^n &= AD_0^n C_0^n + AD_1^n C_1^n + \cdots + AD_{n-1}^n C_{n-1}^n + AD_n^n C_n^n \\ &= \frac{1}{2} AD_0^{n-1} P_0^{n-1}(1) C_0^n \\ &\quad + \frac{1}{2} AD_0^{n-1} P_0^{n-1}(1) C_1^n + \frac{1}{2} AD_1^{n-1} P_1^{n-1}(1) C_1^n \\ &\quad + \cdots \\ &\quad + \frac{1}{2} AD_{n-2}^{n-1} P_{n-2}^{n-1}(1) C_{n-1}^n + \frac{1}{2} AD_{n-1}^{n-1} P_{n-1}^{n-1}(1) C_{n-1}^n \\ &\quad + \frac{1}{2} AD_{n-1}^{n-1} P_{n-1}^{n-1}(1) C_n^n \\ &= \sum_{i=0}^{n-1} AD_i^{n-1} P_i^{n-1}(1) \left(\frac{C_i^n + C_{i+1}^n}{2} \right) \end{aligned} \tag{F.8.2}$$

Q.E.D.

the terminal nodes of nine representative paths in Figure F.1 can be partitioned, after sorted in an ascending order, as {{{35,6}}, {{35,14},{35,14}}, {{35,18},{35,18},{35,18}}, {{35,21},{35,21}}, {{35,29}}} and the number of paths in each partition is the same as the trinomial coefficients of {1, 2, 3, 2, 1}[11]. This relationship always holds at each key state space for the arbitrary number of term segments.

Figure F.2 shows the plot of one-month spot rates in 243 (3^5) representative paths after applying different calibration scheme respectively. The time horizon is 10 years and we use five segments of (0, 11), (12, 35), (36, 59), (60, 83) and (84, 119) in monthly step size. The left panel shows the monthly spot rates after calibration using the first scheme. The calibrated interest rates are very similar to the interest rates before calibration since the LPS bond pricing error is small. The tree is still recombining under the first calibration scheme since the same amount is added to or subtracted from all the interest rate paths at the same time while the tree is no longer recombine under the second calibration scheme as in the right panel.

Figure F.2. One-Month Spot Rates after Different Calibration Schemes

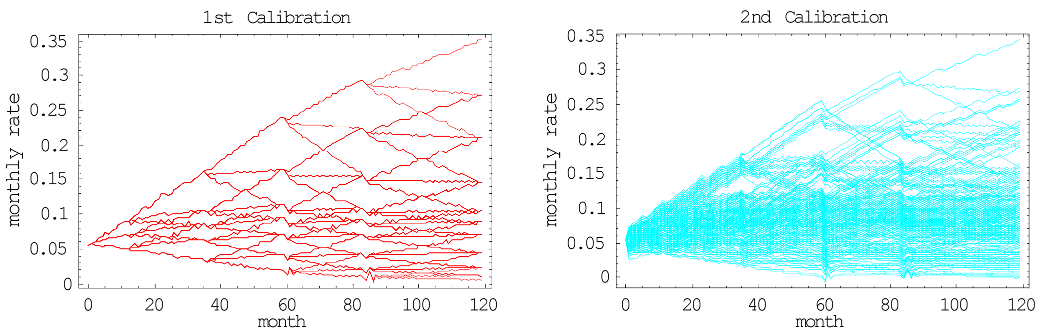

Table F.1 below shows the option pricing error when we use the second calibration method and average out the option payoffs by the weight of binomial coefficient. The option pricing errors, especially for the out-of-the-money options, remarkably decrease compared with those of LPS model without calibration.

Table F.1. Option Pricing Errors of LPS Model when we use the Second Calibration and Average Option Payoffs

Call on a Twenty-Year Zero-Coupon Bond Expiring in Ten Years

[11] The trinomial coefficient can be calculated by $\binom{n}{k}_2 = \sum_{j=0}^{n} (-1)^j \binom{n}{j}\binom{2n-2j}{n-k-j}$,
where $n = 2$ and $k = \{-2, -1, 0, 1, 2\}$ if we use two term segments.

Strike	#Paths	Roll Back	LPS	Error
50	243	0.458153	0.446948	-0.0244561
40	243	2.2722	2.25074	-0.00944515
30	243	5.8127	5.78419	-0.00490619
20	243	10.1269	10.0921	-0.00343984
10	243	14.5134	14.4786	-0.00240213

Call on a Ten-Year Zero-Coupon Bond Expiring in Five Years

Strike	#Paths	Roll Back	LPS	Error
70	27	0.490581	0.486527	-0.00826246
60	27	3.94581	3.93179	-0.00355284
50	27	10.1909	10.1719	-0.00187215
40	27	16.9201	16.9006	-0.00115586
30	27	23.6569	23.6374	-0.000826726
20	27	30.3937	30.3742	-0.000643499
10	27	37.1305	37.111	-0.00052676

Whether we use the first or the second calibration scheme depends on the payoff structure of the financial derivatives as one might expect. If we are to price either pure discount bond or straight coupon bond which has the state-independent payoff structure at maturity, assuming there is no default risk, then the first calibration method will do even though the state price inconsistency still prevails after calibration. And it could be reasonable to discard the unimportant representative paths by linearly ordering them according to the path probability to the extent of not losing the convergence property of the model price since the first calibration method preserves the original LPS structure very well. But when it comes to option pricing, the state prices matter since the option payoff is state-dependent. Therefore, when we are to price option embedded securities such as interest rate option, bond option, etc., we have to use the second calibration method and match the weighted average option payoffs with each representative path in the corresponding key state space partition. And we should be more careful not to throw out the baby with the bathwater by linear-ordering and discarding the paths having a meaningful weight in their role under the second calibration method. Not that the effect of which calibration methods we choose is relatively larger when we use the small number of term segments of LPS model.[12]

[12] Another method of reducing the pricing error of LPS model is to increase the number of term segments instead of calibration.

References

Alexander, C., 2001, Market Models: A Guide to Financial Data Analysis, John Wiley & Sons, Ltd.

Boyle, P and M. Hardy, 2003, Guaranteed Annuity Options, *Astin Bulletin*, Vol.33, No.2, pp.125-152.

Chu, C. C., and Y. K. Kwok, 2005, Valuation of Guaranteed Annuity Options in Affine Term Structure Models, *Working Paper*, Hong Kong University of Science and Technology.

Cox, J.C., S. Ross, and M. Rubinstein, 1979, Option Pricing: A Simplified Approach, *Journal of Financial Economics*, Vol.7, 229-264.

Derman, E., and N. N. Taleb, 2005, The Illusions of Dynamic Replication, *Quantitative Finance*, Vol.5, No.4, pp.323-326.

Diz, F., 1993, Pricing Contingent Claims on a Risky Asset and Stochastic Interest Rates: A New Discrete Time Approach, *Financial Research*, Vol.28, No.1, pp.45-75.

Harrison, J. M., and D. M. Kreps, 1979, Martingales and Arbitrage in Multiperiod Securities Markets, *Journal of Economic Theory*, Vol.20, No.3, pp.381-408.

Heath, D., R. Jarrow, and A. Morton, 1990, Bond Pricing and the Term Structure of Interest Rates: A Discrete Time Approximation, *Journal of Financial and Quantitative Analysis*, Vol.25, No.4, pp.419-440.

Hilliard, J. E., A. L. Schwartz, and A. L. Tucker, 1996, Bivariate Binomial Options Pricing with Generalized Interest Rate Processes, *Journal of Financial Research*, Vol.19 , No.4, pp.585-602.

Ho, T. S. Y., 1992, Managing Illiquid Bonds and The Linear Path Space, *Journal of Fixed Income*, Vol.2, No.1, pp.80-94.

Ho, T. S. Y., 1992, Key Rate Durations: Measures of Interest Rate Risks, *Journal of Fixed Income*, Vol. 2, No. 2, pp.29-44.

Ho, T. S. Y., 1993, Primitive Securities: Portfolio Building Blocks, *Journal of Derivatives*, Vol.1, No.2, pp.6-22.

Ho, T. S. Y., and M. Z. H. Chen, 1997, Arbitrage-free Bond Canonical Decomposition, In: F. Fabozzi (ed.), Advances in Fixed Income Valuation, Frank Fabozzi Associate.

Ho, T. S. Y., and S. B. Lee, 1986, Term Structure Movements and Pricing Interest Rate Contingent Claims, *Journal of Finance*, Vol.41, No.5, pp.1011-1029.

Ho, T. S. Y., and S. B. Lee, 2004, The Oxford Guide to Financial Modeling, Oxford University Press.

Ho, T. S. Y., and S. B. Lee, 2004, A Closed-Form Multifactor Binomial Interest Rate Model, *Journal of Fixed Income*, Vol.14, No.1, pp.8-16.

Ho, T. S. Y., and S. B. Lee, 2005, A Multi-Factor Binomial Interest Rate Model with State-Time-Dependent Volatilities, *Working Paper*, Thomas Ho Company Ltd.

Ho, T. S. Y., S. B. Lee, and Y. S. Choi, 2005, Practical Considerations in Managing Variable Annuities, *Working Paper*, Thomas Ho Company Ltd.

Ho, T. S. Y., and B. Mudavanhu, 2005a, Decomposing and Managing Multivariate Risks: The Case of Variable Annuities, *Journal of Investment Management*, Vol.3, No.4, pp.68-86.

Ho, T. S. Y., and B. Mudavanhu, 2005b, Managing Stochastic Volatility Risks of Interest Rate Options: Key Rate Vega, *Working Paper*, Thomas Ho Company Ltd.

Hull, J. C., 2003, *Options, Futures, and Other Derivatives*, 5th ed., Prentice Hall.

Hull, J., and A. White, 1988, The Use of the Control Variate Technique in Option Pricing, *Journal of Financial and Quantitative Analysis*, Vol.23, No.3, pp.237-251.

Jabbour, G. M., M. V. Kramin, and S. D. Young, 2001, Two-State Option Pricing: Binomial Models Revisited, *Journal of Futures Markets*, Vol.21, No.11, pp.987-1001.

Kao, D., 1996, Default Risk-Based Pricing in a Two-Asset Setting, In: T. S. Y Ho (ed.), *Fixed Income Solutions: New Techniques for Managing market Risks*, (Chicago, IL): Irwin, pp.97-116.

Kao, D., and Y. Geyman, 1995, Immunization Strategy and Pathwise Valuation, In T. S. Y. Ho (ed.), *Fixed Income Investment: Recent Research*, (Irwin: Burr Ridge, IL): 1995, pp. 85-102.

Kishimoto, N., 1989, Pricing Contingent Claims under Interest Rate and Asset Price Risk, *Journal of Finance*, Vol.44, pp.571-589.

Lardic, S., P. Priaulet, and S. Priaulet, 2003, PCA of the Yield Curve Dynamics: Questions of Methodologies, *Journal of Bond Trading and Management*, Vol.1, No.4, pp.327-349.

Lee, S. B., and Y. S. Choi, 2005, Extended Linear Path Space Model, *Working Paper*, Hanyang University.

Lesseig, V., and D. Stock, 1998, The Effect of Interest Rates on the Value of Corporate Assets and the Risk Premia of Corporate Debt, *Review of Quantative Finance and Accounting*, Vol.11, pp.5-22.

Lesseig, V., and D. Stock, 2000, Impact of Correlation of Asset Value and Interest Rates upon Duration and Convexity of Risky Debt, *Journal of Business Research*, Vol.49, pp.289-301.

Milevsky, M. A., and S. D. Promislow, 2001, Mortality Derivatives and the Option to Annuitise, *Insurance: Mathematics and Economics*, Vol.29, pp.299-318.

Nelson, D. B., and K. Ramaswamy, 1990, Simple Binomial Processes as Diffusion Approximations in Financial Models, *Review of Financial Studies*, Vol.3, No.3, pp.393-340.

Pelsser, A., 2003, Pricing and Hedging Guaranteed Annuity Options via Static Option Replication, *Insurance: Mathematics and Economics*, Vol.33, pp.283-296.

Pohlman, L., Wolf, A., and Ho, T. S. Y., 1993, Note on "Managing illiquid bonds and the linear path space"; Response, *Journal of Fixed Income*, Vol.3, No.3, pp.80-88.

Reitano, R. R., 1990, Non-Parallel Yield Curve Shifts and Durational Leverage, *Journal of Portfolio Management*, Vol.16, pp.62-67.

Reitano, R. R., 1995, Two Paradigms for the Market Value of Liabilities, *North American Actuarial Journal*, Vol.1, No.4, pp.104-122.

Rendleman, R. J. and B. J. Bartter, 1979, Two-State Option Pricing, *Journal of Finance*, Vol.34, No.5, pp.1093-1110.

Vasicek, O., 1977, An Equilibrium Characterization of the Term Structure, *Journal of Financial Economics*, Vol.5, No.2, pp.177-188.

Wei, J. Z., 1993, Valuing American Equity Options with a Stochastic Interest Rate: A Note, *Journal of Financial Engineering*, Vol.2, No.2, pp.195-206.

Wilkie , A. D., H. R. Waters, S. Y. Yang, 2003, Reserving, Pricing, and Hedging for Policies with Guaranteed Annuity Options, *British Actuarial Journal*, Vol.9, No.2, pp.263-391.